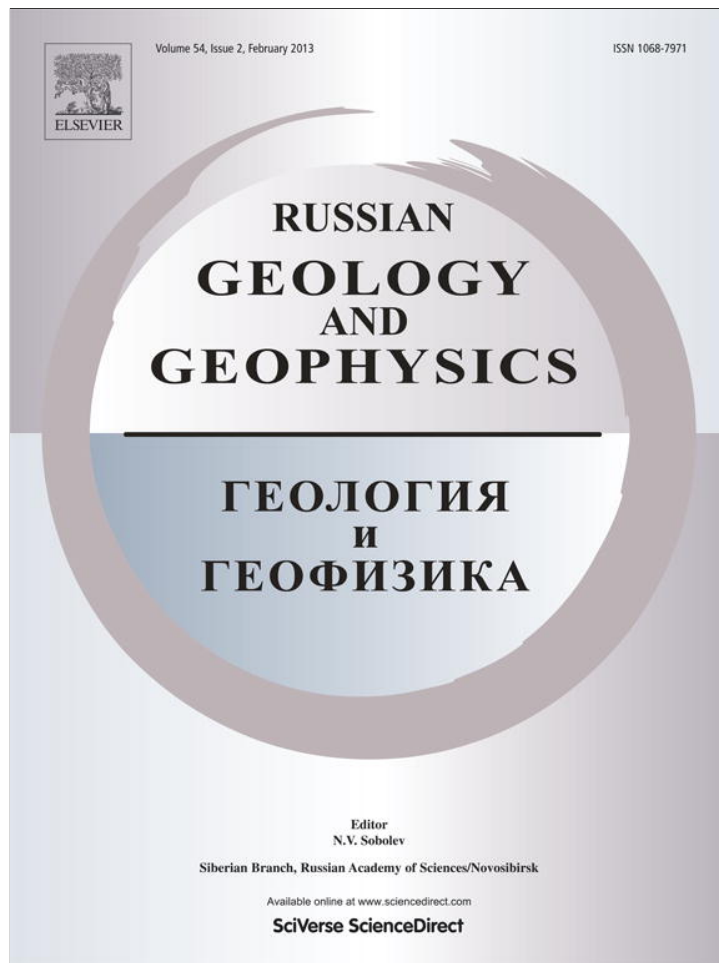


Provided for non-commercial research and education use.
Not for reproduction, distribution or commercial use.



This article appeared in a journal published by Elsevier. The attached copy is furnished to the author for internal non-commercial research and education use, including for instruction at the authors institution and sharing with colleagues.

Other uses, including reproduction and distribution, or selling or licensing copies, or posting to personal, institutional or third party websites are prohibited.

In most cases authors are permitted to post their version of the article (e.g. in Word or Tex form) to their personal website or institutional repository. Authors requiring further information regarding Elsevier's archiving and manuscript policies are encouraged to visit:

<http://www.elsevier.com/copyright>



Self-consistent pressure scales based on the equations of state for ruby, diamond, MgO, B2–NaCl, as well as Au, Pt, and other metals to 4 Mbar and 3000 K

T.S. Sokolova^{a,*}, P.I. Dorogokupets^a, K.D. Litasov^{b,c}

^a *Institute of the Earth's Crust, Siberian Branch of the Russian Academy of Sciences, ul. Lermontova 128, Irkutsk, 664033, Russia*

^b *Novosibirsk State University, ul. Pirogova 2, Novosibirsk, 630090, Russia*

^c *V.S. Sobolev Institute of Geology and Mineralogy, Siberian Branch of the Russian Academy of Sciences, pr. Akademika Koptyuga 3, Novosibirsk, 630090, Russia*

Received 17 April 2012; accepted 14 August 2012

Abstract

Based on the modified formalism of Dorogokupets and Oganov (2007), we calculated the equation of state for diamond, MgO, Ag, Al, Au, Cu, Mo, Nb, Pt, Ta, and W by simultaneous optimization of the data of shock-wave experiments and ultrasonic, X-ray diffraction, dilatometric, and thermochemical measurements in the temperature range from ~100 K to the melting points and pressures of up to several Mbar, depending on the material. The obtained room-temperature isotherms were adjusted with a shift of the R1 luminescence line of ruby, which was measured simultaneously with the unit cell parameters of metals in the helium and argon pressure media. The new ruby scale is expressed as $P(\text{GPa}) = 1870 \cdot \Delta\lambda / \lambda_0 (1 + 6 \cdot \Delta\lambda / \lambda_0)$. It can be used for correction of room-pressure isotherms of metals, diamond, and periclase. New simultaneous measurements of the volumes of Au, Pt, MgO, and B2–NaCl were used for interrelated test of obtained equations of state and calculation of the room-pressure isotherm for B2–NaCl. Therefore, the constructed equations of state for nine metals, diamond, periclase, and B2–NaCl can be considered self-consistent and consistent with the ruby scale and are close to a thermodynamic equilibrium. The calculated *PVT* relations can be used as self-consistent pressure scales in the study of the *PVT* properties of minerals using diamond anvil cell in a wide range of temperatures and pressures.

© 2013, V.S. Sobolev IGM, Siberian Branch of the RAS. Published by Elsevier B.V. All rights reserved.

Keywords: equations of state; pressure scales; ruby pressure scale; diamond; Ag; Al; Au; Cu; Mo; Nb; Pt; Ta; W; MgO; B2–NaCl

Introduction

Significant progress in study of the *PVT* properties of minerals and other materials as applied to the investigation of the Earth's core and mantle has been achieved in recent decades (Bassett, 2009; Hemley and Percy, 2010). For example, in study of perovskite to postperovskite transition and iron structures in the Earth's core, which was carried out in diamond anvil cell with laser heating, the measured temperatures exceeded 3000–5000 K at 150–350 GPa (Hirose et al., 2008; Komabayashi et al., 2008; Tateno et al., 2009, 2010). On the room-temperature isotherm, the measured pressures exceeded 560 GPa (Dubrovinsky et al., 2012; Ruoff et al., 1992). Sakai et al. (2011b) presented the results of numerous measurements of the Fe, Ni, Mo, and NaCl compressibility at

>300 GPa. One of the most crucial problems in such studies is correct measurement of pressure. Unfortunately, there are no barometers for direct measurements in this pressure region. Therefore, pressure in diamond anvil cells is calibrated using special scales, proposed based on the equations of state (EOSs) for materials with a known dependence of pressure on volume and temperature. The EOSs for Au, Pt, MgO, and NaCl and the ruby pressure scale are most commonly used for this purpose.

Most of the EOSs for Au, Pt, MgO, and NaCl that are used as pressure scales were constructed based on the shock compression data (Al'tshuler et al., 1987; Anderson et al., 1989; Carter et al., 1971; Decker, 1971; Hixson and Fritz, 1992; Holmes et al., 1989; Jamieson et al., 1982), using the Mie–Grüneisen–Debye formalism. In this case, however, the difference in pressures determined by different scales reaches 10 GPa in the region of >100 GPa at ~2000 K (Dorogokupets and Oganov, 2007; Fei et al., 2007; Hirose et al., 2008; Shim

* Corresponding author.

E-mail address: sokolovats@crust.irk.ru (T.S. Sokolova)

et al., 2002). A choice of pressure scales depends on the experimental conditions and is determined not by strict thermodynamic approaches but by the individual preference of the research team. For example, Sakai et al. (2011a), who studied the EOS for B2-NaCl at ≤ 304 GPa, chose the EOS for Pt as a pressure scale. They compared the pressures calculated with four EOSs for Pt by Holmes et al. (1989), Fei et al. (2007), Dorogokupets and Oganov (2007), and Matsui et al. (2009) and concluded that the EOS with room-temperature isotherm (Matsui et al., 2009) specified by the Birch–Murnaghan equation is the best pressure scale. At the same time, Matsui et al. (2009) constructed this EOS by analysis of shock compression data and their own measurements of the platinum cell parameters at ≤ 1600 K and ≤ 42 GPa, calibrated against pressure scale based on the EOS for MgO (Matsui et al., 2000). The EOS for MgO (Matsui et al., 2000) was constructed by the methods of molecular dynamics and presented only as a table of the values of $x = V/V_0$ as a function of pressure and temperature, up to 100 GPa and 3000 K. Its parameterization was not published, which does not permit it to be used as a pressure scale, though the pressure can be calculated from the table data, if necessary. Nevertheless, the EOSs for Pt and MgO in this case can be considered consistent with each other, but this gives rise to the question whether the EOS for MgO theoretically obtained by Matsui et al. (2000) is valid.

There are many EOSs for MgO calculated by different methods. Some of them are based only on shock compression data (Jamieson et al., 1982; Jin et al., 2010, 2011; Molodets et al., 2006); others, on results of shock wave, thermochemical, X-ray diffraction, and ultrasonic measurements (Brosh et al., 2008; Dorogokupets and Dewaele, 2007; Dorogokupets and Oganov, 2007; Garai et al., 2009; Gerya et al., 1998, 2004; Hama and Suito, 1999; Jacobs and de Jong, 2003; Jacobs and Oonk, 2000; Kennett and Jackson, 2009; Kuskov et al., 1982; Pan'kov and Kalinin, 1974; Polyakov and Kuskov, 1994; Speziale et al., 2001; Stamenkovic et al., 2012; Stixrude and Lithgow-Bertelloni, 2005; Tange et al., 2009); and in the rest, results of theoretical calculations are corrected using experimental data (Anderson and Zou, 1989; Inbar and Cohen, 1995; Isaak et al., 1990; Otero-de-la-Rosa and Luana, 2011a,b; Wu et al., 2008; Zhang and Bukowinski, 1991). There is also an EOS for MgO that was constructed only by the results of ultrasonic measurements (Spetzler, 1970). Several EOSs for MgO were obtained by X-ray diffraction (Dewaele et al., 2000; Fei, 1999; Martinez-Garcia et al., 2000; Utsumi et al., 1998). Recently, an independent EOS for MgO has been constructed (Kono et al., 2010) (i.e., without using other scales) by simultaneous measurement of sound velocity and X-ray diffraction measurements of the cell parameters at ≤ 1650 K and ≤ 23.6 GPa.

Almost all from the above-mentioned EOSs for MgO can be used as a pressure scale for measurements in diamond anvil cells or in multianvil apparatuses. However, here, as in the case of the EOS presented by Matsui et al. (2000), the question arises of which of them yields the most reliable pressure estimate. Moreover, though periclase in the B1 structure is

stable up to multimegabar pressures and temperatures of several thousand degrees (Belonoshko et al., 2010; Oganov and Dorogokupets, 2003), its single crystals and polycrystalline samples differ in experimentally measured properties, as evidenced from shock compression data (Carter et al., 1971; Duffy and Ahrens, 1995; Zhang et al., 2008), results of ultrasonic measurements (Chung and Simmons, 1969; Fukui et al., 2008; Spetzler, 1970), and X-ray diffraction measurements in diamond anvil cells in the helium pressure medium ensuring quasi-hydrostatic conditions (Jacobsen et al., 2008; Speziale et al., 2001) (see Fig. 5 in (Dorogokupets, 2010)). Therefore, the EOSs for MgO cannot be chosen as a primary pressure scale.

Thus, a question arises: What can serve as a basis for constructing pressure scales? In the megabar pressure region, this is shock adiabats of metals, which can be used to calculate (with particular approximations) the metal isotherms at 0 or 300 K and correlate them with each other. At lower temperatures, the pressure can be calculated from results of simultaneous measurement of the sound velocity and X-ray diffraction. Such procedures were performed for MgO on the room-temperature isotherm (Li et al., 2006) and at higher temperatures (Kono et al., 2010). As yet, similar measurements for metals that are commonly used as pressure scales have not been carried out.

Therefore, the most logical way to obtain internally consistent pressure scales is to calculate metal isotherms at room-temperature from results of shock-wave measurements and compare them with results of independent measurements in diamond anvil cells in the same pressure region. At the same time, an opposite viewpoint was suggested by Holzapfel (2010): The EOSs for metals should be constructed on the basis of low-temperature ultrasonic measurements. In recent time, the EOSs based on thermochemical, ultrasonic, and X-ray diffraction measurements at zero pressure and on shock compression experiments at high pressures (Tange et al., 2009; Yokoo et al., 2009), i.e., without using secondary pressure scales, have again attracted considerable interest. Tange et al. (2009) argue that such EOSs solve the problem of measuring absolute pressure in diamond anvil cells at high temperatures and pressures.

Such isotherms, taken individually, do not solve the problem of consistent pressure scales. First of all, they must be compared with each other at least on the room-temperature isotherm, as was made earlier (Chijioke et al., 2005b; Dewaele et al., 2004b, 2008; Dorogokupets and Oganov, 2006, 2007), to obtain a sufficient number of statistical data. We also showed (Sokolova and Dorogokupets, 2011) that the same shock compression data (Yokoo et al., 2008, 2009) can be used to obtain several EOSs for Au, which almost do not differ in formal features but yield different pressures on isotherms.

We propose the following scheme of obtaining near-absolute (in this work we use the term “optimized”) pressure scales for quasi-hydrostatic conditions (such conditions exist in diamond anvil cells with noble gases as a pressure medium as well as in high-temperature experiments with laser annealing to reduce deviatoric stress): (1) using results of thermo-

chemical, ultrasonic, and X-ray diffraction measurements at zero pressure and of high-pressure shock wave experiments, the EOSs for diamond, periclase, Al, Cu, Nb, Mo, Ag, Ta, W, Pt, and Au are constructed by the formalism (Sokolova and Dorogokupets, 2011) with the minimum set of fitting parameters; (2) with the room-temperature isotherms obtained in the measurements (Dewaele et al., 2004a,b, 2008; Jacobsen et al., 2008; Occelli et al., 2003; Speziale et al., 2001; Takemura and Dewaele, 2008; Takemura and Singh, 2006; Tang et al., 2010), a pressure dependence of the shift of the R1 luminescence line of ruby is constructed; (3) using this calibration plot for ruby, the room-temperature isotherms of other materials are corrected; (4) new EOSs based on the corrected isotherms are constructed; and (5) the obtained EOSs are tested by independent methods.

Thermodynamic model

The Helmholtz free energy of metals in its classical form (Zharkov and Kalinin, 1968) is expressed as:

$$F = U_r + E_r(V) + F_{th}(V, T) - F_{th}(V, T_r) + F_e(V, T) - F_e(V, T_r) + F_{anh}(V, T) - F_{anh}(V, T_r), \quad (1)$$

where U_r is reference energy, $E_r(V)$ is the potential (cold) part of free energy on the reference isotherm T_r (which depends only on volume V), $F_{th}(V, T)$ is the thermal part of Helmholtz free energy (which depends on volume and temperature), and $F_e(V, T)$ and $F_{anh}(V, T)$ are the contributions of free electrons and intrinsic anharmonicity to the free energy, respectively (which depend on V and T).

The pressure on the room-temperature isotherm is determined from the equation proposed by Holzapfel (2001, 2010):

$$P_r(V) = 3K_0 X^{-5} (1 - X) \exp[c_0(1 - X)] \cdot [1 + c_2 \cdot X(1 - X)], \quad (2)$$

where $X = (V/V_0)^{1/3}$, $c_0 = -\ln(3K_0/P_{FG0})$, $P_{FG0} = 1003.6 \times (nZ/V_0)^{5/3}$, $K' = 3 + 2(c_0 + c_2)/3$, V is volume (cm^3/mol), V_0 is volume under standard conditions ($T = 298.15$ K, $P = 1$ bar), n is the number of atoms in the chemical formula, $K_0 = -V(\partial P/\partial V)_T$ is the isothermal bulk modulus (GPa) under standard conditions, $K' = dK_0/dP$, and Z is the atomic number.

The atomic number of elements in compounds is determined from (Knopoff, 1965):

$$Z^{2/3} = \frac{\sum n_i Z_i^{5/3}}{\sum n_i Z_i}, \quad (3)$$

where n_i is the number of atoms i with atomic number Z_i , according to the chemical formula.

Equation (2) is used because it is interpolation between low pressure ($x \geq 1$) and infinite-compression range ($x = 0$) corresponding to the Thomas–Fermi model. Therefore, it is an analog of the Debye and Einstein models, which interpolate thermodynamic functions from 0 K to high temperatures. Differentiating Eq. (2) with respect to volume yields isothermal bulk modulus $K_T = -V(\partial P/\partial V)_T$. Differentiating Eq. (2)

with respect to volume (using numerical methods) yields energy $E_r(V)$ in Eq. (1).

In the physics of metals, an equation proposed by Vinet et al. (1987) is widely used, which determines $E_r(V)$, $P_r(V)$, $K_{T_r}(V)$, and K' as

$$E(V) = 9K_0 V_0 \eta^{-2} \{1 - [1 - \eta(1 - y)] \exp[(1 - y)\eta]\}, \quad (4.1)$$

$$P(V) = 3K_0 y^{-2} (1 - y) \exp[(1 - y)\eta], \quad (4.2)$$

$$K_T(V) = K_0 y^{-2} [1 + (\eta y + 1)(1 - y)] \exp[(1 - y)\eta], \quad (4.3)$$

$$K' = \frac{1}{3} \left[2 + y\eta + \frac{y(1 - \eta) + 2y^2\eta}{1 + (1 - y)(1 + y\eta)} \right], \quad (4.4)$$

where $y = x^{1/3}$ and $\eta = 1.5(K' - 1)$.

As shown earlier (Dorogokupets, 2010; Dorogokupets and Dewaele, 2007), thermodynamic functions at >300 K can be calculated using the Debye or Einstein model. For a more precise calculation of entropy, let us apply the Einstein model with two characteristic temperatures and write the thermal part of Helmholtz free energy as

$$F_{th}(V, T) = m_1 R T \ln \left(1 - \exp \frac{-\theta_1}{T} \right) + m_2 R T \ln \left(1 - \exp \frac{-\theta_2}{T} \right) - \frac{3}{2} n R e_0 x^g T^2, \quad (5)$$

where θ_1 and θ_2 are characteristic temperatures depending on volume and temperature, which permits the intrinsic anharmonicity to be taken into account; $x = V/V_0$; n is the number of atoms in the chemical formula of compound; $m_1 + m_2 = 3n$; e_0 determines the contribution of electrons to the free energy; g is an electronic analog of the Grüneisen parameter; and R is the gas constant.

The dependence of characteristic temperatures on volume and temperature can be expressed (Dorogokupets and Oganov, 2004) as:

$$\theta = \theta(V, T) = \theta(V) \exp \left(\frac{1}{2} a T \right) = \theta(V) \exp \left(\frac{1}{2} a_0 x^m T \right), \quad (6)$$

$$\text{where } a = \left(\frac{\partial \ln \theta(V, T)}{\partial T} \right)_V \text{ and } m = \frac{d \ln a}{d \ln V}.$$

For simplicity, we use one characteristic temperature in the next equations. Differentiating Eq. (5) with respect to temperature at constant volume, we obtain entropy and the thermal part of free energy:

$$S = - \left(\frac{\partial F}{\partial T} \right)_V = 3nR \left[-\ln \left(1 - \exp \frac{-\theta}{T} \right) + \frac{\theta/T}{\exp(\theta/T) - 1} \times \left(1 - \frac{1}{2} a_0 x^m T \right) \right] + 3n R e_0 x^g T, \quad (7)$$

$$E_{th} = F_{th} + TS = 3nR \left[\frac{\theta}{\exp(\theta/T) - 1} \times \left(1 - \frac{1}{2} a_0 x^m T \right) \right] + \frac{3}{2} n R e_0 x^g T^2. \quad (8)$$

Differentiating Eq. (5) with respect to volume at constant temperature, we obtain thermal pressure:

$$P_{th} = - \left(\frac{\partial F_{th}}{\partial V} \right)_T = 3nR \frac{\gamma - \frac{m}{2} a_0 x^m T}{V} \left[\frac{\theta}{\exp(\theta/T) - 1} \right] + \frac{3}{2} nR e_0 x^g T^2 \frac{g}{V}. \quad (9)$$

Thus, using only the first derivatives, we obtained pressure and entropy. Differentiating Eq. (8) with respect to temperature at constant volume and Eq. (9) with respect to volume at constant temperature, we obtain isochoric heat capacity and isothermal bulk modulus:

$$C_V = \left(\frac{\partial E}{\partial T} \right)_V = 3nR \left[\left(\frac{\theta}{T} \right)^2 \frac{\exp(\theta/T)}{[\exp(\theta/T) - 1]^2} \times \left(1 - \frac{1}{2} a_0 x^m T \right)^2 - \frac{(1/4)(a_0 x^m)^2 T \theta}{\exp(\theta/T) - 1} \right] + 3nR e_0 x^g T, \quad (10)$$

$$K_{T_{th}} = -V \left(\frac{\partial P_{th}}{\partial V} \right)_T = -3nR \left[\frac{\theta}{\exp(\theta/T) - 1} \times \frac{q\gamma - \gamma}{V} - \frac{\gamma\theta}{V(\exp(\theta/T) - 1)} \left(\gamma - \frac{m}{2} a_0 x^m T \right) + \frac{\gamma\theta^2 \exp(\theta/T)}{VT(\exp(\theta/T) - 1)^2} \left(\gamma - \frac{m}{2} a_0 x^m T \right) + \frac{m}{2} a_0 x^m T \frac{\theta}{V(\exp(\theta/T) - 1)} \left(\gamma - \frac{m}{2} a_0 x^m T \right) - \frac{m}{2} a_0 x^m \frac{\theta^2 \exp(\theta/T)}{V(\exp(\theta/T) - 1)^2} \left(\gamma - \frac{m}{2} a_0 x^m T \right) - \frac{m}{2} a_0 x^m T \frac{\theta(m-1)}{V(\exp(\theta/T) - 1)} - \frac{1}{2} e_0 x^g T^2 (1-g) \frac{g}{V} \right]. \quad (11)$$

Differentiating Eq. (11) with respect to temperature at constant volume, we obtain

$$\left(\frac{\partial P}{\partial T} \right)_V = 3nR \left[\frac{\frac{1}{2} a_0 x^m \theta (\gamma - m - \frac{1}{2} a_0 x^m m T)}{V(\exp(\theta/T) - 1)} + \frac{\theta^2 (\gamma - \frac{1}{2} a_0 x^m m T) (1 - \frac{1}{2} a_0 x^m T) \exp(\theta/T)}{T^2 V (\exp(\theta/T) - 1)^2} + e_0 x^g T \frac{g}{V} \right]. \quad (12)$$

Now it is easy to calculate the coefficient of thermal expansion, $\alpha = (\partial P / \partial T)_V / K_T$, heat capacity at constant pressure, $C_P = C_V + \alpha^2 TVK_T$, and adiabatic bulk modulus $K_S = K_T + VT(\alpha K_T)^2 / C_V$, which can also be obtained by direct

experimental methods. Enthalpy and Gibbs free energy are determined from the formulas $H = E + PV$ and $G = F + PV$.

The pressure on the shock adiabat is calculated by the equation from (Zharkov and Kalinin, 1968):

$$P_H = \frac{P(V) - \frac{\gamma}{V} [E(V) - E(V_0)]}{1 - \gamma(1-x)/(2x)}. \quad (13)$$

As seen from Eqs. (9), (11), (12), and (13), two new parameters have appeared: $\gamma = - \left(\frac{\partial \ln \theta}{\partial \ln V} \right)_T$ and $q = \left(\frac{\partial \ln \gamma}{\partial \ln V} \right)_T$, whose dependence on volume has not been determined yet. In the previous works (Dorogokupets, 2002, 2007, 2010; Dorogokupets and Dewaele, 2007; Dorogokupets and Organov, 2003, 2006, 2007) we used the dependence $\gamma = \gamma_\infty + (\gamma_0 - \gamma_\infty) x^\beta$ (Al'tshuler et al., 1987), where γ_0 is the Grüneisen parameter under standard conditions, γ_∞ is the Grüneisen parameter on infinite compression ($x = 0$), and β is the fitting parameter. However, this equation is rather flexible. There are direct equations relating the Grüneisen parameter to volume on isotherms at 0 or 300 K. The relation on the 0 K isotherm is expressed (Burakovsky and Preston, 2004; Zharkov and Kalinin, 1968) as

$$\gamma = \frac{\frac{K'}{2} - \frac{1}{6} - \frac{t}{3} \left(1 - \frac{P}{2K} \right)}{1 - \frac{2tP}{3K}} + \delta, \quad (14)$$

where t can be equal to 0, 1, and 2, which corresponds to the Slater, Dugdale–MacDonald, and Zubarev–Vashchenko models, respectively, and δ is the additive normalizing constant.

Zharkov and Kalinin (1968) obtained three variants of the EOS for metals and other materials with three fixed values of t , but we will use the latter as an fitting parameter. If t does not depend on volume and $\delta = 0$, then, the characteristic temperature, depending on volume, can be calculated from the simple equation:

$$\theta = \theta_0 x^{1/6} K_0^{-1/2} (K - 2tP/3)^{1/2}, \quad (15)$$

or by the numerical integration of Eq. (14), if $\delta \neq 0$. Thus, we determined all thermodynamic functions necessary to construct the EOSs. The procedure of optimization of fitting parameters is described in our previous work (Dorogokupets and Organov, 2007).

Let us consider in more detail the correlation between the obtained relations and the shock compression data. The classical methods for calculating isotherms at 0 or 300 K and normal adiabats (isentropes) from shock-wave data are well known (Al'tshuler et al., 1987; Fortov and Lomonosov, 2010; Ruoff, 1967; Zharkov and Kalinin, 1968). The velocity of shock wave, U_S (km/s), and mass velocity of material behind the shock front, U_P (km/s), are in linear or quadratic relations:

$$U_S = a_0 + a_1 U_P \text{ or } U_S = a_0 + a_1 U_P + a_2 U_P^2. \quad (16)$$

The pressure (GPa) and volume on the shock adiabat are determined from the equations (c_0 in g/cm^3):

$$P_H = \rho_0 U_P U_S, \quad x = \rho_0 / \rho = V / V_0 = (U_S - U_P) / U_S. \quad (17)$$

Coefficients a_0 and a_1 in Eq. (13) are related to adiabatic bulk modulus K_{S_0} and its pressure derivative (Al'tshuler et al., 1987; Ruoff, 1967; Zharkov and Kalinin, 1968) as follows:

$$K_S = \rho_0 a_0^2, \quad (\partial K_S / \partial P)_S = 4a_1 - 1. \quad (18)$$

Here the problem arises: How can we find parameters K_0 and K' determining the room-temperature isotherm from the known shock adiabat parameters under standard conditions, Eq. (16)? Parameters K_0 and K_{S_0} are related to each other by the equation $K_S = K_T + VT(\alpha K_T)^2 / C_V$, which can also be expressed as $\frac{1}{K_S} = \frac{1}{K_T} - \frac{\alpha^2 VT}{C_P}$. The coefficient of thermal expansion, volume, and heat capacity at constant pressure under standard conditions are known for most materials; therefore, it is not difficult to calculate K_0 from K_S , which can be obtained from ultrasonic measurements.

To obtain K' consistent with $(\partial K_S / \partial P)_S$ from the shock compression data, let us use the relation (Ruoff, 1967)

$$(\partial K_S / \partial P)_S = (\partial K_S / \partial P)_T + \gamma (\partial \ln K_S / \partial \ln T)_P. \quad (19)$$

All the above relations can be calculated from our EOS. Earlier we optimized the above system of equations so that the shock pressure and calculated value of $(\partial K_S / \partial P)_S$ would be consistent with shock adiabat in Eq. (13) and Eqs. (16)–(18) (Dorogokupets and Sokolova, 2011; Sokolova and Dorogokupets, 2011). But this approximation is too strict because the shock adiabat can also be expressed via quadratic relation in Eq. (16). Therefore, in this work we refused this approximation and used a smooth adiabat calculated from Eqs. (16) and (17) and a shock pressure estimated from Eq. (13).

The equations of state based on results of thermochemical, ultrasonic, and X-ray diffraction measurements and shock compression data

Parameter a_0 in Eq. (16) was calculated based on the most reliable and generally accepted values of K_{S_0} obtained in

ultrasonic measurements (Table 1), which made it possible to correlate them with the shock compression data for standard conditions. Using the shock compression database (Levashov et al., 2004) and data of later measurements (Yokoo et al., 2008, 2009; Zhang et al., 2008), we again calculated a_1 in Eq. (16). Both parameters were invoked to calculate the smooth adiabats used for optimization. The accepted values of a_0 and a_1 , adiabatic bulk modulus, and its pressure derivative as well as the reference values of volume, density, and atomic number are listed in Table 1.

The optimization parameters of the EOSs in thermochemical, ultrasonic, and X-ray diffraction measurements and the shock compression data are listed in Tables 2 and 3. Optimization was made by two models. In the first model, the room-temperature isotherm was specified by Eq. (2) (Holzapfel, 2001, 2010) (Table 2), and in the second, by Eq. (4.2) (Vinet et al., 1987) (Table 3). The models show no significant difference, but the second yields higher values of K' . Both models smooth the measured isobaric heat capacity at ≥ 100 K; therefore, the calculated standard entropy is close to the reference values. It is remarkable that one of the characteristic temperatures is close to the Debye temperature, whereas the other is usually twice as low. The tables present the values of parameters $(\partial K_S / \partial P)_T$ and $(\partial K_S / \partial P)_S$ calculated from our EOSs. They are not always close to the values obtained from the shock compression data (Table 1). This evidences that the velocities are usually related to each other by quadratic rather than linear equations. The degree of consistence of the calculated thermodynamic functions with the experimental data obtained for the studied materials by the first model using Eq. (2) (Holzapfel, 2001, 2010) was considered by Dorogokupets et al. (2012). Figure 1 shows the calculated thermodynamic functions of periclase in comparison with the results of direct experimental measurements. The second model using Eq. (4.2) (Vinet et al., 1987) yields nearly the same degree of consistence.

As seen from the example with periclase (Fig. 1), we described rather accurately all major thermodynamic functions, using a simple EOS with the minimum set of fitting parameters. Now it is necessary to reduce the EOSs for metals and compounds, otherwise any of them can be considered absolute. We will do this first of all on the room-temperature

Table 1. Input parameters of shock adiabats of studied materials

Parameters	C	MgO	Al	Cu	Nb	Mo	Ag	Ta	W	Pt	Au
$V_0, \text{cm}^3/\text{mole}$	3.414	11.248	9.98	7.112	10.828	9.369	10.25	10.861	9.552	9.091	10.215
$\rho_0, \text{g/cm}^3$	3.518	3.583	2.704	8.935	8.58	10.240	10.524	16.66	19.25	21.46	19.282
$a_0, \text{km/s}$	11.21	6.733	5.295	3.923	4.48	5.05	3.14	3.40	4.01	3.62	2.995
a_1	1.20	1.30	1.361	1.506	1.18	1.27	1.645	1.25	1.262	1.543	1.653
$a_2, \text{km/s}$	–	–	–	–	–	–	–	–	–	–	–0.013
K_{S_0}, GPa	442.0	162.5	75.9	137.4	172.1	261.7	103.9	193.0	309.7	281.2	173.0
$(\partial K_S / \partial P)_S$	3.80	4.20	4.44	5.02	3.74	4.08	5.58	4.0	4.05	5.17	5.61
Z	6	10.34	13	29	41	42	47	73	74	78	79

Table 2. Parameters of the equations of state, optimizing results of thermochemical, ultrasonic, and X-ray measurements and shock compression data.

Parameter	C	MgO	Al	Cu	Nb	Mo	Ag	Ta	W	Pt	Au
K_0 , GPa	441.5	160.3	72.8	133.5	170.5	260.0	100.0	191.0	308.0	275.3	167.0
K'	3.98	4.23	4.56	5.27	3.63	4.17	6.16	3.91	4.10	5.21	5.79
$(\partial K_S / \partial P)_T$	3.977	4.20	4.40	5.24	3.61	4.15	6.12	3.89	4.08	5.15	5.67
$(\partial K_S / \partial P)_S$	3.973	4.16	4.26	5.14	3.58	4.12	5.97	3.86	4.06	5.07	5.54
θ_{10} , K	1560	749	381	298	296	369	197	235	310	163	176
m_1	2.437	3	1.5	1.5	1.5	1.5	1.5	1.5	1.5	1.5	1.5
θ_{20} , K	684	401	202	168	136	213	115	109	172	153	84.5
m_2	0.563	3	1.5	1.5	1.5	1.5	1.5	1.5	1.5	1.5	1.5
t	1.140	0.555	-0.861	1.417	-0.829	-0.655	2.253	-0.279	-0.564	-0.890	-0.512
δ	-0.537	-0.226	-0.247	0	-0.354	-0.686	0.175	-0.205	-0.642	0	0
a_0 (10^{-6} K $^{-1}$)	–	14.6	–	–	–	–	–	–	–	–	–
m	–	5.3	–	–	–	–	–	–	–	–	–
e_0 (10^{-6} K $^{-1}$)	0	–	64.1	27.7	114.6	143.1	17.6	80.7	100.3	75.5	0
g	–	–	0.66	0.66	0.98	2.65	0.62	0.2	2.70	0.32	–

Note. Isotherm at 300 K is specified by Eq. (2) (Holzapfel, 2001, 2010).

Table 3. Parameters of the equations of state, optimizing results of thermochemical, ultrasonic, and X-ray measurements and shock compression data.

Parameter	C	MgO	Al	Cu	Nb	Mo	Ag	Ta	W	Pt	Au
K_0 , GPa	441.5	160.3	72.8	133.5	170.5	260.0	100.0	191.0	308.0	275.3	167.0
K'	4.00	4.38	4.70	5.44	3.77	4.32	6.02	4.08	4.25	5.28	5.81
$(\partial K_S / \partial P)_T$	3.99	4.35	4.55	5.41	3.75	4.29	5.99	4.06	4.23	5.23	5.71
$(\partial K_S / \partial P)_S$	3.99	4.31	4.40	5.31	3.72	4.26	5.86	4.03	4.21	5.16	5.58
θ_{10} , K	1549	747	380	297	305	419	201	247	313	169	179
m_1	2.468	3	1.5	1.5	1.5	1.5	1.5	1.5	1.5	1.5	1.5
θ_{20} , K	669	401	202	168	132	190	116	104	169	150	83.5
m_2	0.532	3	1.5	1.5	1.5	1.5	1.5	1.5	1.5	1.5	1.5
t	1.367	1.064	-0.451	2.172	-0.171	-0.342	2.722	0.330	-0.259	-0.102	0.164
δ	-0.470	-0.165	-0.182	0.136	-0.183	-0.512	0.442	-0.073	-0.557	0.278	0.254
a_0 (10^{-6} K $^{-1}$)	–	16.5	–	–	–	–	–	–	–	–	–
m	–	4.96	–	–	–	–	–	–	–	–	–
e_0 (10^{-6} K $^{-1}$)	0	–	64.1	27.7	116.5	150.4	19.2	82.1	104.3	78.5	0
g	–	–	0.61	2.27	0.89	1.94	0.56	0.100	2.29	0.26	–

Note. Isotherm at 300 K is specified by Eq. (4.2) (Vinet et al., 1987).

isotherm by calibrating the ruby pressure scale against the room-temperature isotherms from Tables 2 and 3.

Calibration of the ruby pressure scale against the equations of state for other materials

In recent decade, the cell parameters of the considered materials and the shift of the R1 luminescence line of ruby have been measured in diamond anvil cells in the helium pressure medium. As shown by Takemura (2001), using helium as a pressure medium ensures a hydrostatic pressure

of at least 50 GPa, and at higher pressures, helium ensures quasi-hydrostatic conditions (Dewaele et al., 2004a,b, 2008; Klotz et al., 2009; Occelli et al., 2003). This problem was reviewed in detail by Syassen (2008).

The ruby pressure scale was repeatedly calibrated under nonhydrostatic conditions (Mao et al., 1978), in the argon (Mao et al., 1986) and helium pressure media (Aleksandrov et al., 1987; Chijioke et al., 2005b; Dewaele et al., 2004b, 2008; Dorogokupets and Oganov, 2003, 2006, 2007; Jacobsen et al., 2008; Holzapfel, 2003; Silvera et al., 2007; Syassen, 2008). Our new calibration of the ruby pressure scale is based on the EOSs for materials that were constructed using the

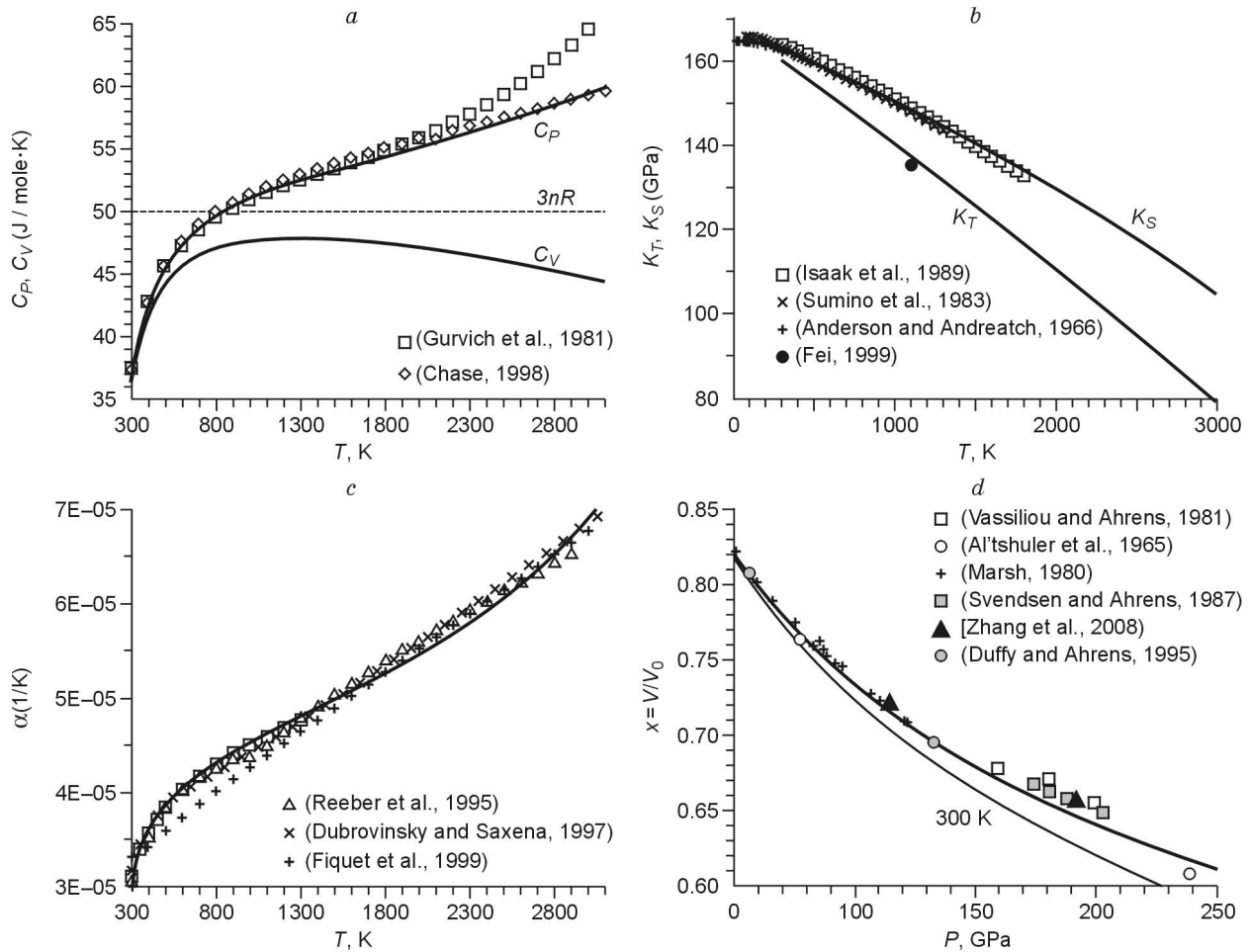


Fig. 1. Thermodynamic functions of MgO (solid lines). (a) Calculated heat capacity (isobaric and isochoric) in comparison with selected reference and experimental data. (b) Calculated bulk moduli (isothermal (K_T) and adiabatic (K_S)) in comparison with that from ultrasonic measurements. (c) Calculated coefficient of volumetric thermal expansion in comparison with experimental data. (d) Calculated shock compression adiabat in comparison with experimental data. Thin line is a room-temperature isotherm constructed from the parameters in Table 2.

same formalism with thermochemical, ultrasonic, and X-ray diffraction measurements at zero pressure as well as shock compression data at high pressures. It is expressed as

$$P \text{ (GPa)} = 1870 \frac{\Delta \lambda}{\lambda_0} \left(1 + 6.0 \frac{\Delta \lambda}{\lambda_0} \right), \quad (20)$$

where $\lambda_0 = 694.24$ nm.

This scale is based on the EOSs for 11 materials and averages the scales obtained by the equations of Holzapfel (2001, 2010) and Vinet et al. (1987). It was described in detail earlier (Dorogokupets et al., 2012). The comparison between the modern ruby scales and the scale proposed by Mao et al. (1986) shows that at 150 GPa, the latter scale underestimates pressure by 10–15 GPa (Fig. 2).

Let us correct the room-temperature isotherms with the ruby scale (Eq. 20) and again consider the EOSs for the studied materials. This is necessary because the shock adiabat does not correspond to equilibrium thermodynamic functions (Zharkov and Kalinin, 1968 (section 5.1); Holzapfel, 2010 (section 11)). Among our isotherms, there are probably ones

close to the equilibrium isotherms as well as nonequilibrium ones. Therefore, the ruby pressure scale averages the room-temperature isotherms of studied materials, based on the results of thermochemical, ultrasonic, and X-ray diffraction measurements at zero pressure and shock compression measurements at high pressures.

The optimized equations of state under quasi-hydrostatic conditions

The parameters of the optimized EOSs are presented in Table 4. They were obtained as follows. First, the room-temperature isotherms were corrected with the ruby scale by Eq. (20). Then, optimization of the results of thermochemical, ultrasonic, and X-ray diffraction measurements and shock compression data was repeated for the fixed room-temperature isotherms (K_0 and K' for (2) (Holzapfel, 2001)). This procedure was performed for all studied materials, but the EOSs for Au, Pt, and MgO were studied in more detail because they

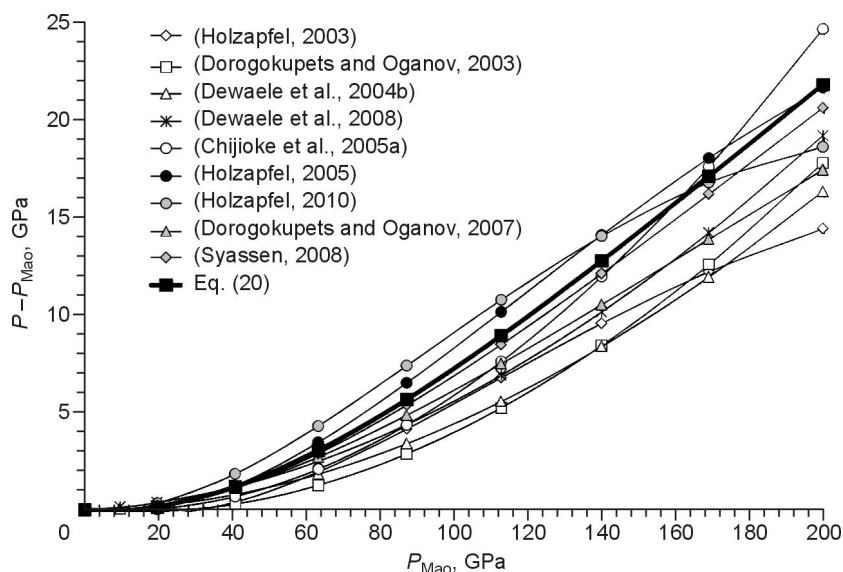


Fig. 2. Difference between the recent calibrations of the ruby pressure scales (P) and the classic ruby pressure scale (Mao et al., 1986) (P_{Mao}). Pressure was calculated from the parameters in the original work by Mao and by Eq. (20).

are the most demanded pressure scales for experiments in high-pressure multianvil apparatuses.

The difference between the ruby pressure scale and the corrected room-temperature isotherms is shown in Fig. 3. A comparison shows that the pressures of almost all studied materials are characterized by a ~2% deviation in the region of quasi-hydrostatic compression. The only exclusion is gold. In the region of hydrostatic compression (<50 GPa), the pressure deviation is most often >2%. The 1.5 GPa deviations for Al, Mo, and Ta in the pressure region of ~30 GPa are unexpected and call for additional experimental analysis.

Verification of the equations of state by the independent determination

The EOSs for MgO, Au, and Pt have been the most widely discussed as possible pressure scales in the recent decade. We have already performed their optimization (Dorogokupets and Dewaele, 2007; Dorogokupets and Oganov, 2006, 2007). The proposed approach to the construction of EOSs and the published new data of simultaneous measurements of the volume of these materials (Dewaele et al., 2008; Hirose et al., 2008; Komabayashi et al., 2008; Kono et al., 2010; Matsui et

Table 4. Optimized parameters of the equations of state

Parameter	C	MgO	Al	Cu	Nb	Mo	Ag	Ta	W	Pt	Au
K_0 , GPa	441.5	160.3	72.8	133.5	170.5	260.0	100.0	191.0	308.0	275.0	167.0
K'	3.90	4.10	4.51	5.32	3.65	4.20	6.15	3.83	4.12	5.35	5.90
$(\partial K_S / \partial P)_T$	3.90	4.07	4.35	5.28	3.62	4.17	6.10	3.81	4.10	5.29	5.81
$(\partial K_S / \partial P)_S$	3.89	4.03	4.21	5.18	3.60	4.15	5.96	3.79	4.08	5.22	5.68
θ_{10} , K	1561	748	381	296	302	353	199	254	309	177	179.5
m_1	2.436	3	1.5	1.5	1.5	1.5	1.5	1.5	1.5	1.5	1.5
θ_{20} , K	684	401	202	169	134	222	115	101	172	143	83.0
m_2	0.564	3	1.5	1.5	1.5	1.5	1.5	1.5	1.5	1.5	1.5
t	1.085	0.301	-0.958	1.401	-0.763	-0.791	2.210	-0.148	-0.591	-0.343	0.087
δ	-0.506	-0.235	-0.242	-0.07	-0.326	-0.802	0.178	-0.101	-0.686	0.167	0.134
a_0 (10^{-6} K^{-1})	-	17.4	-	-	-	-	-	-	-	-	-
m	-	4.95	-	-	-	-	-	-	-	-	-
e_0 (10^{-6} K^{-1})	-	-	64.1	27.7	115.9	143.2	22.1	82.3	100.1	80.6	-
g	-	-	0.33	2.18	0.90	2.66	0.19	0.12	2.77	0.06	-

Note. Parameters K_0 and K' are given for Eq. (2).

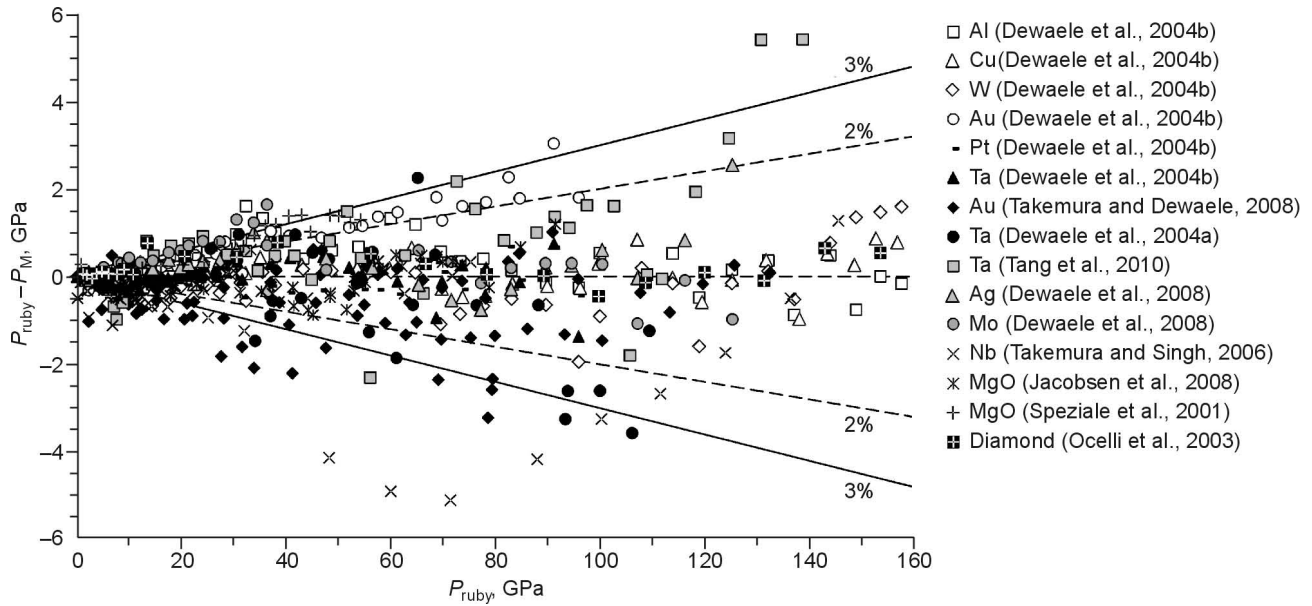


Fig. 3. Difference between the pressure calculated with the ruby scale (P_{ruby} , Eq. (20)) and the pressure on the room-temperature isotherm of metals, diamond, and periclase (P_M) calculated from the parameters in Table 4. The ratios between $\Delta\lambda/\lambda_0$ and $x = V/V_0$ were obtained in experiments in the argon pressure medium (Tang et al., 2010) and in the helium pressure medium (other works).

al., 2009; Takemura and Dewaele, 2008; Sakai et al., 2011a; Sata et al., 2010; Ueda et al., 2008; Yokoo et al., 2008, 2009) permit their correction for better consistency with each other.

This procedure was performed as follows. We compiled a database of simultaneous measurements of the MgO, Au, and Pt volumes on the room-temperature isotherm and at elevated temperatures, introduced them into our EOSs, and inserted the

relations between Excel tables with different EOSs. Unfortunately, this database is not full because the results of many measurements were published only graphically (Dubrovinsky et al., 2010; Fei et al., 2007). Then we calculated the difference between the pressures that yield different EOSs: first, for those on the room-temperature isotherms, and then, for those at high temperatures. Variation in K' values is accompanied by

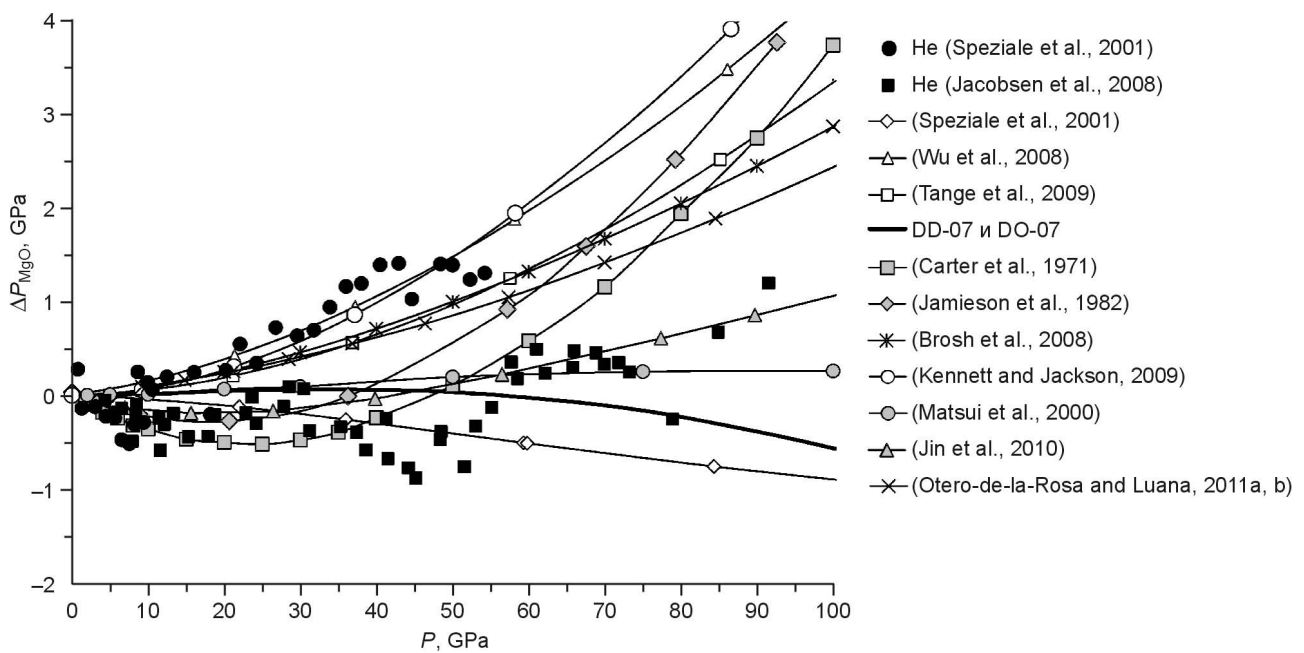


Fig. 4. Difference between the pressures measured in diamond anvil cells in the helium pressure medium (He) (Jacobsen et al., 2008; Speziale et al., 2001) and then recalculated using a ruby pressure scale (Eq. (20)) and the room-temperature isotherm of MgO (the parameters in Table 4). Lines show the difference between the room-temperature isotherms of MgO obtained with the EOSs from the above works and with our EOS (Table 4). DD-07 and DO-07 are the EOSs for MgO proposed by Dorogokupets and Dewaele (2007) and Dorogokupets and Oganov (2007), respectively.

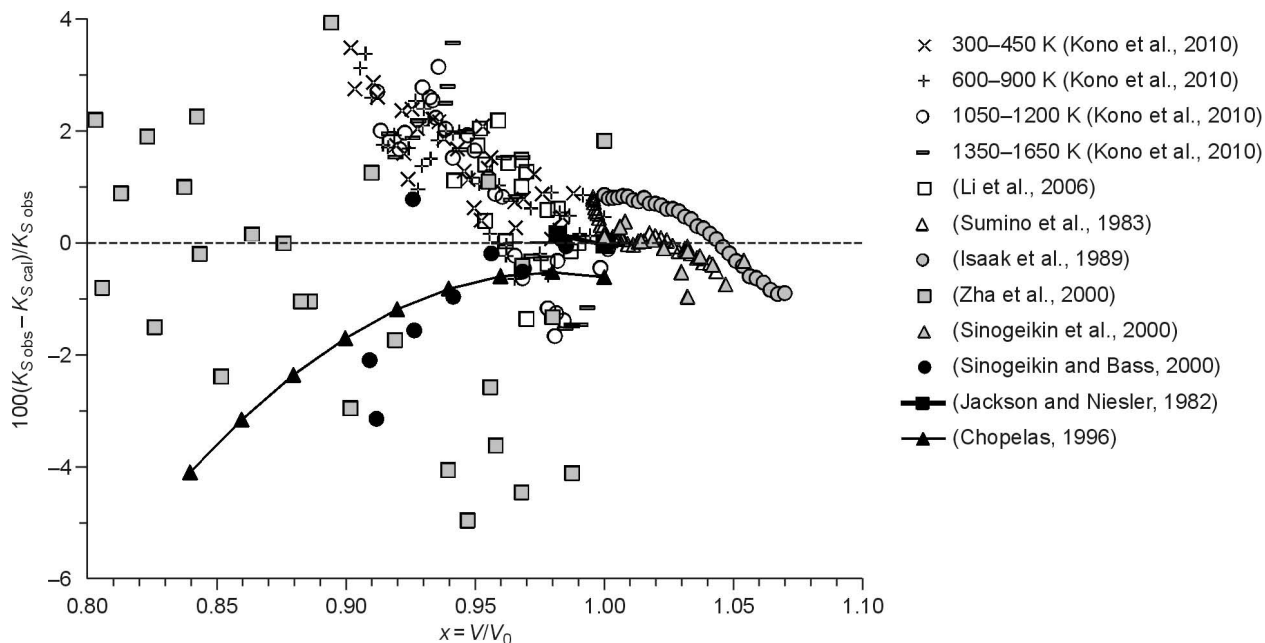


Fig. 5. Difference (in %) between the measured ($K_{S \text{ obs}}$) (Kono et al., 2010) and calculated ($K_{S \text{ cal}}$) (by our EOS (Table 4)) adiabatic bulk moduli of MgO. Measurements in other mentioned works were performed on the room-temperature isotherm.

changes in the relations between the EOSs. At high pressures (>300 GPa), the obtained EOSs for MgO, Au, and Pt were tested by simultaneous measurements of the volumes of these materials and B2–NaCl. As an initial approximation, we took our previous data (Dorogokupets and Dewaele, 2007; Dorogokupets and Oganov, 2006, 2007).

The room-temperature isotherm of MgO agrees with the results of measurements in the helium pressure medium (Jacobsen et al., 2008) (Fig. 4). Up to 100 GPa, it is consistent

only with the EOSs proposed by Jin et al. (2010) and Matsui et al. (2000). Other modern EOSs yield much higher pressures and agree with the results of measurements by Speziale et al. (2001).

Recently, Kono et al. (2010) have obtained an EOS for MgO by simultaneous measurement of sound velocities and X-ray diffraction, without using other scales. Similar procedures were earlier performed by Li et al. (2006) and Zha et al. (2000). Therefore, it was important to obtain an EOS for MgO which would be consistent with the results of not only *PVT* but also direct ultrasonic measurements of the adiabatic bulk modulus.

The difference between the measured adiabatic bulk moduli of MgO and those calculated by the proposed EOS (Table 4) is shown in Fig. 5, and the difference between the pressures from (Kono et al., 2010, Table 1) and our calculated pressures, in Fig. 6. It is seen that our EOS for MgO approximates (with a reasonable accuracy) the results of ultrasonic measurements of the adiabatic bulk modulus. The systematic discordance between the pressures in the measurements by Kono et al. (2010) (Fig. 6) might point out the nonhydrostatic conditions. This is confirmed (Kono et al., 2010; Fig. 8) by the fact that the calculated thermal expansion of MgO disagrees with the direct measurements of the MgO volume (Dubrovinsky and Saxena, 1997; Fiquet et al., 1999) at high temperatures and 1 bar. In general, the calculated adiabatic bulk modulus agrees with the experimental one within 2%, though the discordance between these moduli in the experiments carried out by Zha et al. (2000) reaches 6%.

In Fig. 7, comparison of the EOSs for MgO and Au at ≤ 30 GPa and ≤ 2173 K is made. Most of the *PVT* points calculated from the EOSs for MgO and Au agree with each other within ± 0.5 GPa, and almost all of them are in the

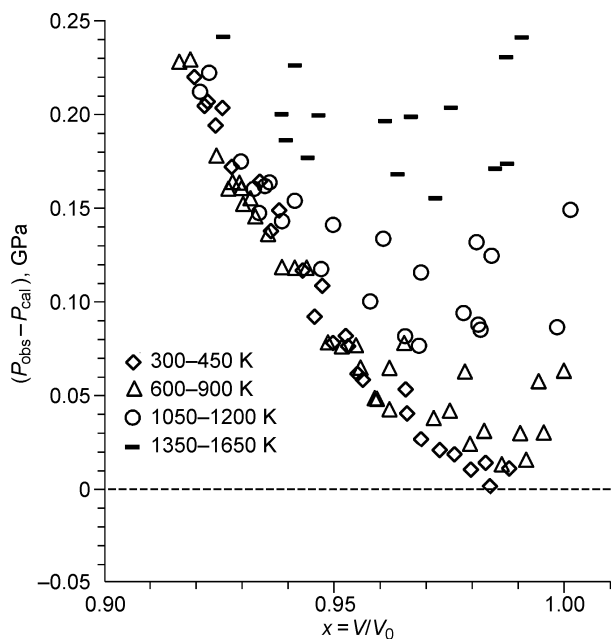


Fig. 6. Difference between the pressures determined from the EOS proposed by Kono et al. (2010) (P_{obs}) and our EOS for MgO (P_{cal}).

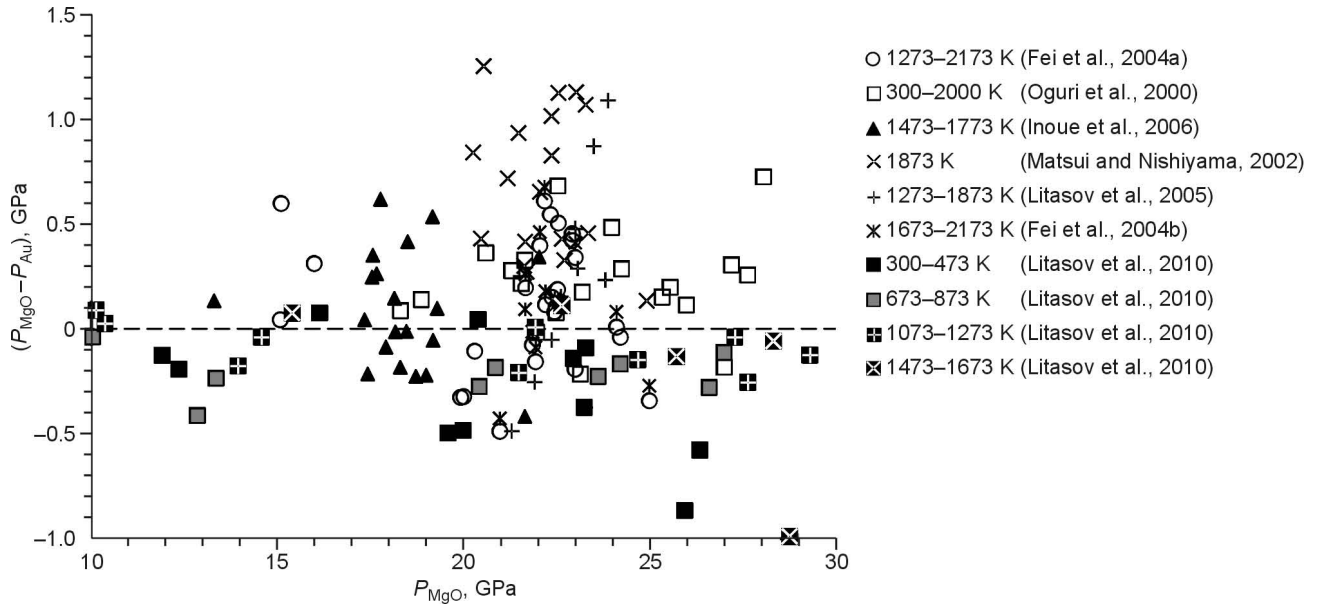


Fig. 7. Difference between the pressures obtained from our EOSs for MgO and Au, calculated from the results of simultaneous measurements of their cell parameters at the given temperature.

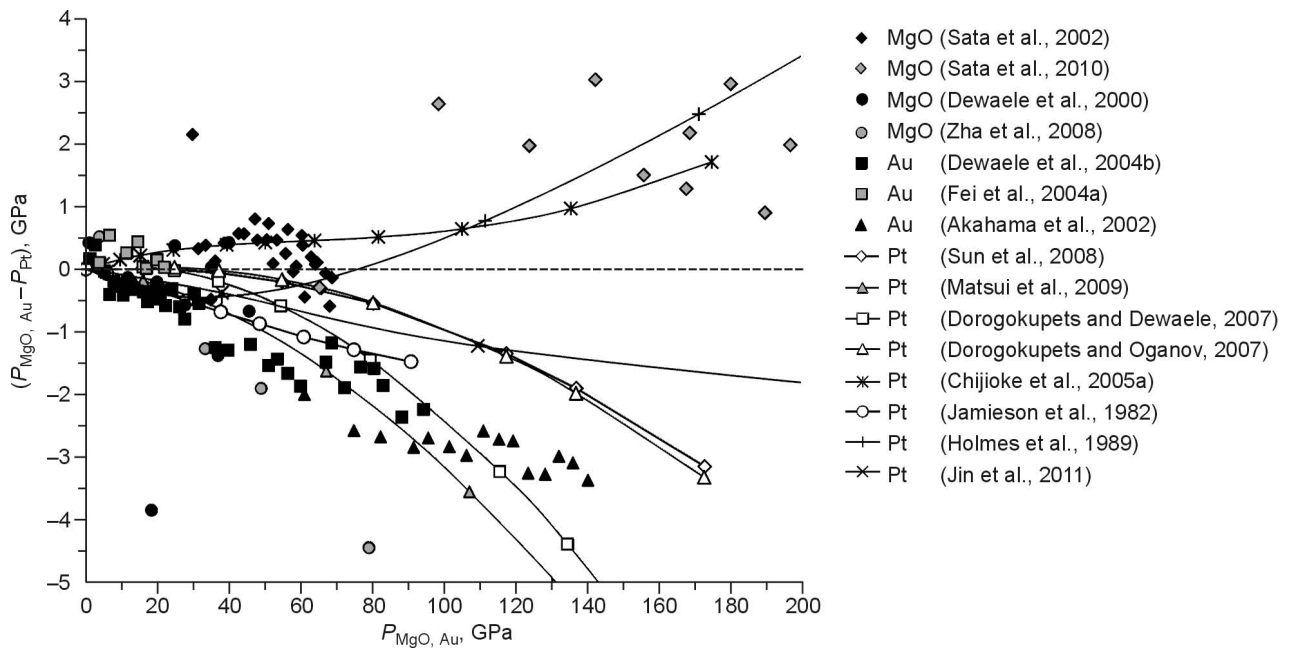


Fig. 8. Difference in pressure between our EOSs for MgO and Au and the EOS for Pt, calculated from the results of simultaneous measurements of the MgO–Pt and Au–Pt cell parameters on the room-temperature isotherm borrowed from literature. Also, the difference between the EOSs for Pt from (Chijioko et al., 2005a; Dorogokupets and Dewaele, 2007; Dorogokupets and Oganov, 2007; Holmes et al., 1989; Jamieson et al., 1982; Jin et al., 2011) and our EOS for Pt is shown.

variation interval of ± 1 GPa. However, the EOSs for MgO and Au differ by >1 GPa at 1873 K (Matsui and Nishiyama, 2002).

Comparison of the EOSs for MgO, Au, and Pt on the room-temperature isotherm at ≤ 200 GPa is shown in Fig. 8. Our isotherm of Pt agrees with the isotherms of other researchers (Chijioko et al., 2005a; Jamieson et al., 1982; Jin

et al., 2011; Holmes et al., 1989) and significantly exceeds our earlier estimates (Dorogokupets and Dewaele, 2007; Dorogokupets and Oganov, 2007) based on nonhydrostatic measurements (Akahama et al., 2002). At high temperatures, the difference in pressures estimated from the EOSs for MgO, Au, and Pt does not exceed 3 GPa, which is close to the error of determination (Fig. 9).

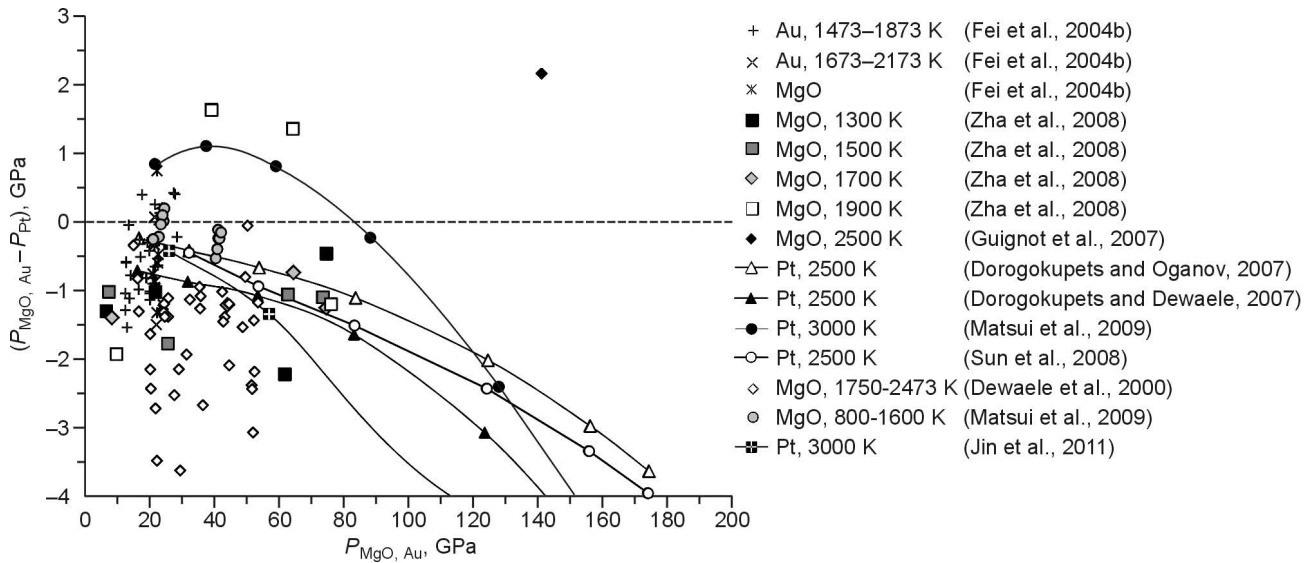


Fig. 9. Difference in pressure between our EOSs for MgO and Au and the EOS for Pt, calculated from the results of simultaneous measurements of the MgO–Pt and Au–Pt cell parameters at high temperatures. Also, the difference between the EOSs for Pt from (Dorogokupets and Dewaele, 2007; Dorogokupets and Oganov, 2007; Jin et al., 2011; Matsui et al., 2009; Sun et al., 2008) and our EOS for Pt is shown.

The B2-NaCl isotherm at 300 K

Results of simultaneous measurements of the volumes of Au, Pt, MgO, and B2-NaCl were published elsewhere (Hirose et al., 2008; Komabayashi et al., 2008; Ono et al., 2006; Sakai et al., 2011a; Sata et al., 2002, 2010; Ueda et al., 2008). They can be used to calculate an isotherm for B2-NaCl at 300 K and verify the EOSs for Au, Pt, and MgO obtained at >300 GPa. Figure 10 shows the compression curve for

B2-NaCl in comparison with direct experimental data recalculated by our EOSs. The data of Heinz and Jeanloz (1984b) are based on the ruby pressure scale (Mao et al., 1978), but laser heating was used to reduce deviatoric stress (which is consistent with the data of other researchers) in only one measurement. The EOS for B2-NaCl (Ueda et al., 2008) agrees with our previous estimates (Dorogokupets and Dewaele, 2007), but they significantly underestimate pressure at >100 GPa.

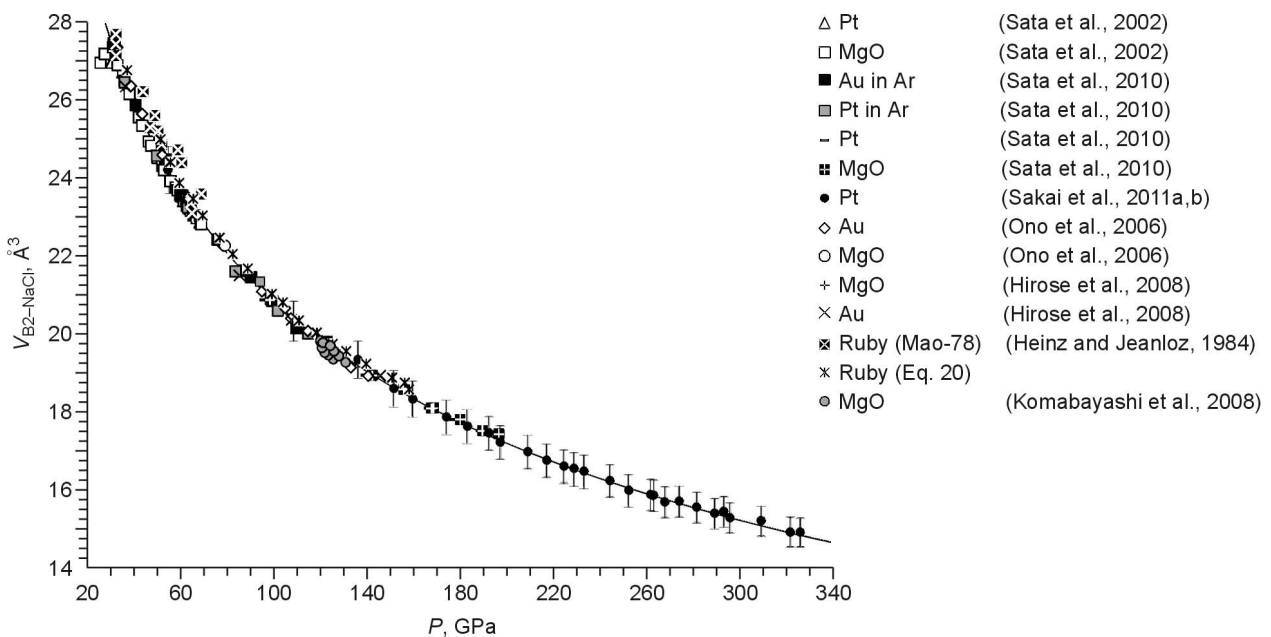


Fig. 10. NaCl compressibility curve on the room-temperature isotherm. Original experimental data were recalculated using our MgO, Pt, Au (Table 4), and hcp-Fe (Dorogokupets et al., 2012) pressure scales. Line is the B2-NaCl isotherm calculated by Eq. (2) with parameters $V_0 = 40.351 \text{ \AA}^3$, $K_0 = 30.2 \text{ GPa}$, and $K' = 5.15$. The error bars for volumes determined by Sakai et al. (2011a,b) are given. Mao-78 is the scale proposed by Mao et al. (1978).

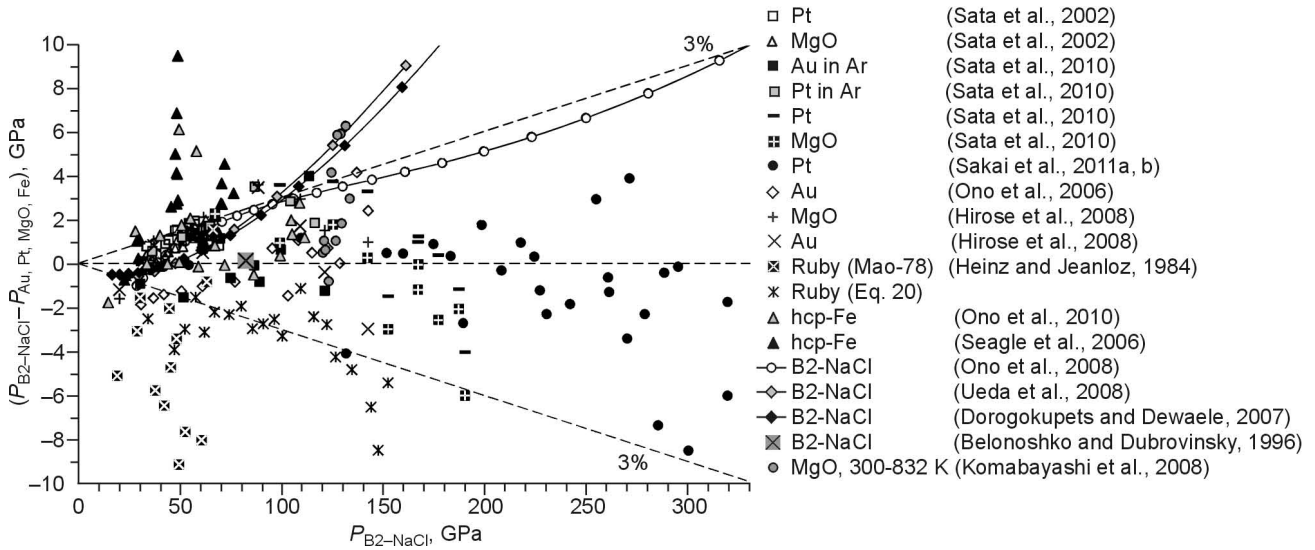


Fig. 11. Difference between the smoothed B2-NaCl isotherm at room-temperature (Fig. 10) and MgO, Pt, Au (Table 4), and hcp-Fe (Dorogokupets et al., 2012) pressure scales, according to the results of measurements from the above-mentioned references. Mao-78 is the scale proposed by Mao et al. (1978). 3%—line of 3% deviation of calculated data.

Figure 11 is the key to verify the room-temperature isotherms for Au, Pt, and MgO, whose parameters are listed in Table 4. The difference in pressure according to the platinum scale (Sakai et al., 2011b) reaches ± 5 GPa, but most of the pressures differ within ± 2 GPa. The gold scale yields a somewhat smaller difference, but it cannot be verified by the ruby scale at >150 GPa because of lack of experimental data. As seen from the figure, the results of almost all measurements made after stress relieving (by the gas pressure medium or laser heating) agree within 3%.

Independent verification of the EOSs for Au, Pt, and B2-NaCl can be made by a simultaneous measurement of sound velocities in B2-NaCl, the volumes of Au, Pt, and B2-NaCl, and the shift of the R1 luminescence line of ruby. Lakshmanov et al. (2005) reported such measurements at 35–73 GPa, but their data have not been published yet.

Independent comparison with other pressure scales

Recently, Dorfman et al. (2012) have published results of comparison of the Au, Pt, Mo, MgO, and B2-NaCl pressure scales up to 265 GPa for the room-temperature isotherm. They made a simultaneous measurement of the volumes of Au and NaCl, MgO and NaCl, Mo and MgO, Pt and MgO, Pt and NaCl, and Pt:NaCl and MgO in diamond anvil cells in the Ne and He pressure media. Therefore, it is of great interest to compare our EOSs with the independent measurements by Dorfman et al. (2012). Figure 12 shows a difference between the pressure calculated from the equation of state proposed by Dorfman et al. (2012) and the pressure calculated from the parameters presented in Table 4. These EOSs are in good agreement, but Dorfman et al. (2012) considerably expanded the pressure range as compared with the previous measurements. Using these data, we can correct our EOSs for MgO,

Au, and Mo. The parameters of the corrected EOSs are as follows: MgO— $K_0 = 160.3$ GPa, $K' = 4.25$, $\theta_{10} = 748$ K, $\theta_{20} = 401$ K, $t = 0.583$, $\delta = -0.25$, $a_0 = 17.4 \times 10^{-6} \text{ K}^{-1}$, $m = 5.5$; Au— $K_0 = 167.0$ GPa, $K' = 5.75$, $\theta_{10} = 176$ K, $\theta_{20} = 84$ K, $t = -0.463$, $\delta = 0.045$; and Mo— $K_0 = 260.5$ GPa, $K' = 4.05$, $\theta_{10} = 356$ K, $\theta_{20} = 218$ K, $t = -0.735$, $\delta = -0.755$, $e_0 = 123.9 \times 10^{-6} \text{ K}^{-1}$, $g = 3.5$. We recommend the following parameters for the room-temperature isotherm of B2-NaCl: $V_0 = 41.00 \text{ \AA}^3$, $K_0 = 27.6$ GPa, $K' = 5.31$, $c_0 = 2.768$ (for Eq. (2)).

Tables 5, 7, and 9 present thermodynamic functions of MgO, Mo, and Au, which were calculated from the corrected parameters of the EOS based on data by Dorfman et al. (2012). They were tabulated against temperature at zero pressure, at 100 GPa, and on compression, $x = V/V_0$ of up to 0.6. The tables present the calculated coefficient of volumetric thermal

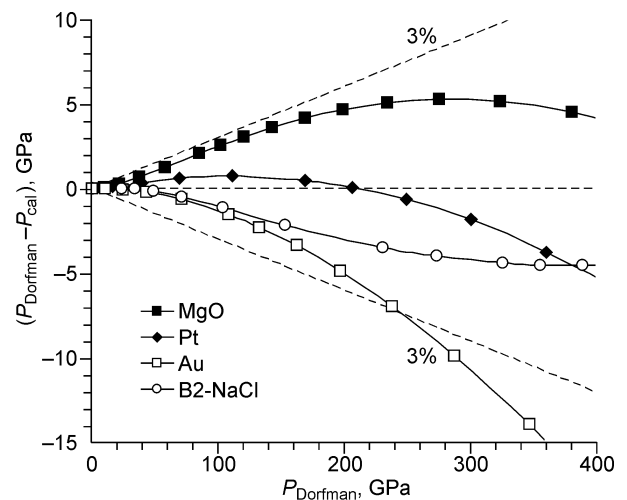


Fig. 12. Difference between the pressures calculated by the pressure scales from Dorfman et al. (2012) and the pressures calculated by the EOSs for MgO, Pt, Au, and B2-NaCl from Table 4.

Table 5. Thermodynamic functions of MgO at different pressures and temperatures, calculated using the EOS of MgO corrected by the data from Dorfman et al. (2012) (see the text).

P , GPa	T , K	$x = V/V_0$	$\alpha E-6$, K^{-1}	S , J mole $^{-1}$ K $^{-1}$	C_P , J mole $^{-1}$ K $^{-1}$	C_V , J mole $^{-1}$ K $^{-1}$	K_T , GPa	K_S , GPa	γ_{th}	K'	ΔG , kJ mole $^{-1}$
0	298.15	1	30.38	26.90	36.95	36.45	160.30	162.48	1.502	4.25	0.000
0	500	1.00705	37.93	48.43	45.45	44.19	154.80	159.22	1.505	4.29	-7.716
0	1000	1.02828	44.59	82.08	51.01	47.78	140.31	149.78	1.514	4.40	-41.153
0	2000	1.08025	54.28	118.91	55.51	47.60	110.44	128.78	1.530	4.73	-143.504
0	3000	1.14778	68.19	142.22	59.91	45.60	79.41	104.32	1.533	5.28	-274.706
100	298.15	0.72633	7.03	13.83	26.33	26.26	518.43	519.66	1.133	3.26	933.854
100	500	0.72764	10.38	30.90	38.85	38.62	514.96	517.99	1.133	3.26	929.300
100	1000	0.73196	12.68	61.22	47.24	46.57	505.31	512.57	1.132	3.27	905.636
100	2000	0.74173	13.63	95.18	50.33	48.83	485.78	500.76	1.131	3.30	825.660
100	3000	0.75208	14.05	115.83	51.47	49.13	466.72	488.94	1.129	3.33	719.496
100	4000	0.76285	14.37	130.75	52.28	49.11	448.34	477.34	1.126	3.36	595.871
235.839	298.15	0.6	3.26	9.06	20.43	20.41	938.20	939.13	1.012	2.97	1934.600
236.694	500	0.6	5.50	23.36	34.48	34.38	937.79	940.40	1.012	2.97	1937.098
239.778	1000	0.6	7.19	51.48	45.40	45.07	938.19	945.01	1.010	2.97	1938.694
246.856	2000	0.6	7.70	84.17	49.29	48.54	941.05	955.63	1.007	2.97	1916.952
254.144	3000	0.6	7.74	104.01	50.35	49.20	944.63	966.65	1.003	2.97	1871.403
261.464	4000	0.6	7.72	118.20	50.93	49.41	948.51	977.78	1.000	2.97	1809.365

Table 6. Volume dependence of Grüneisen parameter and volume- and temperature-depending pressures (GPa) calculated using the parameters of the EOS of MgO corrected by the data from Dorfman et al. (2012) (see the text)

$x = V/V_0$	γ	Temperature, K								
		0	298.15	500	1000	1500	2000	2500	3000	3500
1	1.514	-0.690	0.000	1.104	4.167	7.276	10.337	13.332	16.254	19.100
0.95	1.427	8.538	9.166	10.235	13.267	16.378	19.464	22.501	25.483	28.406
0.9	1.350	20.528	21.101	22.137	25.150	28.276	31.396	34.485	37.532	40.535
0.85	1.281	36.169	36.690	37.695	40.699	43.852	47.018	50.165	53.284	56.371
0.8	1.218	56.684	57.156	58.132	61.137	64.329	67.550	70.766	73.966	77.143
0.75	1.161	83.792	84.218	85.166	88.179	91.422	94.712	98.009	101.298	104.574
0.7	1.108	119.951	120.333	121.251	124.281	127.588	130.962	134.353	137.745	141.132
0.65	1.059	168.745	169.085	169.973	173.027	176.414	179.887	183.390	186.902	190.415
0.6	1.013	235.540	235.839	236.694	239.778	243.261	246.856	250.491	254.144	257.804
0.55	0.970	328.578	328.838	329.658	332.777	336.377	340.117	343.912	347.732	351.566
0.5	0.929	460.960	461.182	461.962	465.121	468.861	472.776	476.764	480.788	484.830

expansion (α), entropy (S), heat capacity at constant pressure (C_P) and at constant volume (C_V), isothermal (K_T) and adiabatic (K_S) bulk moduli, thermodynamic Grüneisen parameter ($\gamma_{th} = \alpha V K_T / C_V = \alpha V K_S / C_P$), parameter K' from Eq. (2), and Gibbs free energy increment relative to the standard state, which coincides with the Gibbs energy increment from the known thermodynamic database (Holland and Powell, 1998, 2011). Tables 6, 8, and 10 present pressure for MgO, Mo, and Au depending on temperature and compression as well as Grüneisen parameter $\gamma = -(\partial \ln \theta / \partial \ln V)_T$ depending on volume.

Conclusions

We have obtained the EOSs for 11 materials, which agree with each other within 2–3% uncertainty. These equations can be considered optimized pressure scales for quasi-hydrostatic conditions on the room-temperature isotherm. They agree both with the ruby scale (Eq. (20)) and with each other, as shown by the example of the EOSs for Au, Pt, and MgO. The EOSs for Au, Pt, and MgO agree with each other not only on the room-temperature isotherm but also at high temperatures, as shown by their intercomparison. Using the room-temperature

Table 7. Thermodynamic functions of Mo at different pressures and temperatures, calculated using the EOS of Mo corrected by the data from Dorfman et al. (2012) (see the text)

P , GPa	T , K	$x = V/V_0$	$\alpha E-6$, K^{-1}	S , J mole $^{-1}$ K $^{-1}$	C_P , J mole $^{-1}$ K $^{-1}$	C_V , J mole $^{-1}$ K $^{-1}$	K_T , GPa	K_S , GPa	γ_{th}	K'	ΔG , kJ mole $^{-1}$
0	298.15	1	14.04	28.55	24.09	23.94	260.50	262.06	1.431	4.05	0.000
0	500	1.00305	15.96	41.55	26.11	25.80	255.99	259.03	1.488	4.06	-7.170
0	1000	1.01205	19.84	60.54	28.90	27.99	242.83	250.69	1.632	4.10	-33.159
0	2000	1.03735	30.58	82.45	35.69	31.93	206.78	231.11	1.924	4.22	-105.531
0	3000	1.08049	55.51	99.27	51.07	37.08	149.43	205.79	2.264	4.44	-196.468
100	298.15	0.78852	4.44	22.31	22.29	22.26	622.36	623.11	0.916	3.37	819.871
100	500	0.78928	5.03	34.48	24.51	24.46	619.89	621.36	0.942	3.37	814.054
100	1000	0.79143	5.78	52.07	26.16	26.01	612.92	616.50	1.011	3.38	791.960
100	2000	0.79655	7.13	70.81	28.11	27.66	595.74	605.46	1.145	3.39	729.555
100	3000	0.80283	8.63	82.59	30.17	29.21	574.09	593.04	1.276	3.41	652.526
100	4000	0.81049	10.41	91.60	32.65	30.85	547.48	579.48	1.403	3.43	565.275
190.789	298.15	0.7	2.78	20.11	21.56	21.55	918.72	919.31	0.777	3.18	1449.759
191.345	500	0.7	3.16	31.96	24.02	23.99	918.45	919.60	0.794	3.18	1448.074
192.896	1000	0.7	3.55	49.16	25.55	25.47	917.69	920.43	0.839	3.18	1437.511
196.412	2000	0.7	4.11	67.20	26.83	26.63	915.36	922.34	0.927	3.18	1401.421
200.416	3000	0.7	4.65	78.18	27.95	27.56	911.86	924.71	1.009	3.18	1354.647
204.896	4000	0.7	5.20	86.23	29.11	28.47	907.18	927.69	1.087	3.18	1301.652

Table 8. Volume-depending Gruneisen parameter and volume- and temperature-depending pressure (GPa) calculated using the parameters of the EOS of Mo corrected by the data from Dorfman et al. (2012) (see the text)

$x = V/V_0$	γ	Temperature, K								
		0	298.15	500	1000	1500	2000	2500	3000	3500
1	1.348	-0.692	0.000	0.784	2.986	5.493	8.294	11.385	14.766	18.436
0.95	1.201	14.199	14.823	15.548	17.585	19.893	22.460	25.282	28.360	31.692
0.9	1.079	33.395	33.964	34.641	36.540	38.680	41.046	43.637	46.450	49.486
0.85	0.975	58.274	58.796	59.433	61.218	63.215	65.411	67.800	70.383	73.159
0.8	0.887	90.741	91.224	91.829	93.519	95.396	97.445	99.661	102.043	104.592
0.75	0.810	133.485	133.935	134.513	136.125	137.903	139.827	141.894	144.104	146.454
0.7	0.743	190.367	190.789	191.345	192.896	194.592	196.412	198.354	200.416	202.596
0.65	0.684	267.064	267.462	268.002	269.505	271.137	272.874	274.712	276.650	278.687
0.6	0.631	372.135	372.512	373.041	374.512	376.095	377.768	379.524	381.362	383.282

Table 9. Thermodynamic functions of Au at different pressures and temperatures, calculated using the EOS of Au corrected by the data from Dorfman et al. (2012) (see the text)

P , GPa	T , K	$x = V/V_0$	$\alpha E-6$, K^{-1}	S , J mole $^{-1}$ K $^{-1}$	C_P , J mole $^{-1}$ K $^{-1}$	C_V , J mole $^{-1}$ K $^{-1}$	K_T , GPa	K_S , GPa	γ_{th}	K'	ΔG , kJ mole $^{-1}$
0	298	1	41.77	47.54	25.39	24.51	167.00	173.05	2.908	5.75	0.000
0	500	1.00883	45.33	60.93	26.46	24.79	157.11	167.65	2.960	5.84	-11.053
0	1000	1.03467	56.93	80.08	29.35	24.91	129.51	152.57	3.128	6.11	-46.774
0	1300	1.05425	69.22	88.11	32.27	24.93	109.49	141.74	3.274	6.35	-72.036
100	298	0.75908	9.71	31.65	23.50	23.37	638.35	642.15	2.056	4.26	866.713
100	500	0.76061	10.21	44.13	24.62	24.37	632.90	639.55	2.060	4.26	858.967
100	1000	0.76459	10.61	61.47	25.34	24.80	619.31	632.89	2.069	4.28	832.091
100	2000	0.77295	11.13	79.27	26.07	24.91	591.80	619.31	2.088	4.32	760.744
100	3000	0.78181	11.68	89.97	26.77	24.93	563.81	605.45	2.109	4.35	675.789
350.386	298	0.6	3.79	21.63	21.42	21.37	1618.86	1622.08	1.761	3.71	2565.984
351.704	500	0.6	4.18	33.33	23.65	23.57	1619.06	1625.02	1.761	3.71	2568.433
355.188	1000	0.6	4.36	50.09	24.78	24.59	1620.34	1632.79	1.761	3.71	2568.476
362.305	2000	0.6	4.40	67.24	25.24	24.85	1623.50	1648.66	1.761	3.71	2552.460
369.456	3000	0.6	4.40	77.33	25.48	24.90	1626.79	1664.61	1.761	3.71	2523.663

Table 10. Volume-depending Gruneisen parameter and volume- and temperature-depending pressure (GPa) calculated using the parameters of the EOS of Au corrected by the data from Dorfman et al. (2012) (see the text)

$x = V/V_0$	γ	Temperature, K							
		0	298.15	500	1000	1500	2000	2500	3000
1	2.908	-1.693	0.000	1.418	4.957	8.504	12.052	15.602	19.151
0.95	2.655	8.350	9.921	11.279	14.677	18.083	21.493	24.903	28.313
0.9	2.454	22.287	23.761	25.080	28.391	31.714	35.040	38.368	41.696
0.85	2.290	41.658	43.051	44.348	47.614	50.896	54.182	57.470	60.758
0.8	2.153	68.683	70.006	71.292	74.547	77.823	81.104	84.388	87.672
0.75	2.036	106.622	107.879	109.164	112.437	115.738	119.046	122.357	125.669
0.7	1.934	160.352	161.547	162.837	166.156	169.511	172.875	176.242	179.612
0.65	1.843	237.344	238.474	239.777	243.165	246.603	250.052	253.507	256.964
0.6	1.761	349.324	350.386	351.704	355.188	358.737	362.305	365.878	369.456
0.55	1.687	515.256	516.243	517.578	521.181	524.877	528.596	532.326	536.060
0.5	1.617	766.887	767.788	769.136	772.884	776.764	780.678	784.606	788.541

isotherms of Au, Pt, and MgO as pressure scales, we obtained a new B2–NaCl isotherm, which can serve as a pressure scale at >300 GPa and is consistent with the Pt pressure scale under these conditions. We also corrected the room-temperature isotherm of hcp-Fe, using the new ruby pressure scale and the EOS for W (Dorogokupets et al., 2012). The high-temperature EOSs for B2–NaCl and hcp-Fe will be considered in a special paper.

Thus, we have obtained the best EOSs for Au, Pt, MgO, and B2–NaCl on the room-temperature isotherm, taking into account the data from Dorfman et al. (2012) and using the second-order equation (Eq. (2)) from Holzapfel (2001, 2010). A subsequent increase in the accuracy of pressure scales based on the EOSs for Au, Pt, MgO, and B2–NaCl is possible but with the use of third-order equations.

The used calculation procedure will also be applied to study the EOSs for silicates, carbonates, and metal compounds obtained recently by our research team for thermodynamic description of phases in the Earth's (Dobretsov and Shatskiy, 2012) and other planets' interior and comparison of results with experimental data on mantle systems, including ones with volatiles (Litasov, 2011). The procedure of calculation of *PVT* relations and phase thermodynamics using the proposed EOSs can be found online at <http://labpet.crust.irk.ru>.

We thank N.V. Sobolev, A.B. Belonoshko, O.G. Kuskov, and O.G. Safonov for great work on reviewing and editing our paper and valuable remarks. We also thank A. Dewaele (CEA, France) for providing unpublished data on the B2–NaCl compressibility.

This work was supported by grants 12-05-00758-a and 12-05-33008 from the Russian Foundation for Basic Research, Project 14.B37.21.0457 from the Ministry of Education and Science of the Russian Federation, and Integration Project 97 (2012-2014) from the Siberian Branch of the Russian Academy of Sciences.

References

- Akahama, Y., Kawamura, H., Singh, A.K., 2002. Equation of state of bismuth to 222 GPa and comparison of gold and platinum pressure scales to 145 GPa. *J. Appl. Phys.* 92, 5892–5897.
- Aleksandrov, I.V., Goncharov, A.F., Zisman, A.N., Stishov, S.M., 1987. Diamond at high pressures: Raman scattering, equation of state, high-pressure scale. *ZhETF* 93, 680–691.
- Al'tshuler, L.V., Trunin, R.F., Simakov, G.V., 1965. Shock compression of periclase and quartz and composition of the Earth's lower mantle. *Izv. Akad. Nauk SSSR. Ser. Fizika Zemli* 29 (10), 1–6.
- Al'tshuler, L.V., Brusnikin, S.E., Kuz'menkov, E.A., 1987. Isotherms and Gruneisen functions of 25 metals. *Prikladnaya Mekhanika i Teoreticheskaya Fizika* 161, 134–146.
- Anderson, O.L., Isaak, D.G., Yamamoto, S., 1989. Anharmonicity and the equation of state of gold. *J. Appl. Phys.* 65, 1534–1543.
- Anderson, O.L., Andreatch, P., 1966. Pressure derivatives of elastic constants of single-crystal MgO at 23 and -195.8 °C. *J. Am. Ceram. Soc. Bull.* 49, 404–409.
- Anderson, O.L., Zou, K., 1989. Formulation of the thermodynamic functions for mantle minerals: MgO as an example. *Phys. Chem. Miner.* 16, 642–648.
- Bassett, W.A., 2009. Diamond anvil cell, 50th birthday. *High Pressure Res.* 29, 163–186.
- Belonoshko, A.B., Dubrovinsky, L.S., 1996. Molecular dynamics of NaCl (B1 and B2) and MgO (B1) melting: two-phase simulation. *Am. Mineral.* 81, 303–316.
- Belonoshko, A.B., Arapan, S., Martonak, R., Rosengren, A., 2010. MgO phase diagram from first principles in a wide pressure-temperature range. *Phys. Rev. B* 81, 054110, doi: 10.1103/PhysRevB.81.054110.
- Brosh, E., Shnek, R.Z., Makov, G., 2008. Explicit Gibbs free energy equation of state for solids. *J. Phys. Chem. Solids* 69, 1912–1922, doi: 10.1016/j.jpcs.2008.01.019.
- Burakovsky, L., Preston, D.L., 2004. Analytic model of the Gruneisen parameter all densities. *J. Phys. Chem. Solids* 65, 1581–1587, doi: 10.1016/j.jpcs.2003.10.076.
- Carter, W.J., Marsh, S.P., Fritz, J.N., McQueen, R.G., 1971. The equation of state of selected materials for high-pressure references, in: Lloyd, E.C. (Ed.), *Accurate Characterization of the High Pressure Environment* (National Bureau of Standards, Washington, DC). NBS Spec. Publ. 326, 147–158.
- Chase, M.W., Jr., 1998. NIST-JANAF thermochemical tables. Fourth Ed. *J. Phys. Chem. Ref. Data*, Monograph 9.

- Chijioke, D., Nellis, W.J., Silvera, I.F., 2005a. High-pressure equations of state of Al, Cu, Ta, and W. *J. Appl. Phys.* 98, 073526, doi: 10.1063/1.2071449.
- Chijioke, D., Nellis, W.J., Soldatov, A., Silvera, I.F., 2005b. The ruby pressure standard to 150 GPa. *J. Appl. Phys.* 98, 114905, doi: 10.1063/1.2135877.
- Chopelas, A., 1996. The fluorescence sideband method for obtaining acoustic velocities at high compressions: application to MgO and MgAl₂O₄. *Phys. Chem. Miner.* 23, 25–37.
- Chung, D.H., Simmons, G., 1969. Elastic properties of polycrystalline periclase. *J. Geophys. Res.* 74, 2133–2135.
- Decker, D.L., 1971. High-pressure equation of state for NaCl, KCl, and CsCl. *J. Appl. Phys.* 42, 3239–3244.
- Dewaele, A., Fiquet, G., Andrault, D., Hausermann, D., 2000. P-V-T equation of state of periclase from synchrotron radiation measurements. *J. Geophys. Res.* 105B, 2869–2877, doi: 10.1029/1999JB900364.
- Dewaele, A., Loubeyre, P., Mezouar, M., 2004a. Refinement of the equation of state of tantalum. *Phys. Rev. B* 69, 092106, doi: 10.1103/PhysRevB.69.092106.
- Dewaele, A., Loubeyre, P., Mezouar, M., 2004b. Equations of state of six metals above 94 GPa. *Phys. Rev. B* 70, 094112, doi: 10.1103/PhysRevB.70.094112.
- Dewaele, A., Torrent, M., Loubeyre, P., Mezouar, M., 2008. Compression curves of transition metals in the Mbar range: experiments and projector augmented-wave calculations. *Phys. Rev. B* 78, 104102, doi: 10.1103/PhysRevB.78.104102.
- Dobretsov, N.L., Shatskiy, A.F., 2012. Deep carbon cycle and geodynamics: the role of the core and carbonatites melts in the lower mantle. *Russian Geology and Geophysics (Geologiya i Geofizika)* 53 (11), 1117–1132 (1455–1475).
- Dorfman, S.M., Prakapenka, V.B., Meng, Y., Duffy, T.S., 2012. Intercomparison of pressure standards (Au, Pt, Mo, MgO, NaCl and Ne) to 2.5 Mbar. *J. Geophys. Res.* 117, B08210, doi:10.1029/2012jb009292.
- Dorogokupets, P.I., 2002. Critical analysis of equations of state for NaCl. *Geochem. Int.* 40 (Suppl. 1), S132–S144.
- Dorogokupets, P.I., 2007. The equation of state of magnesite for the Earth's lower-mantle conditions. *Geokhem. Int.* 45, 561–568.
- Dorogokupets, P.I., 2010. P-V-T equations of state of MgO and thermodynamics. *Phys. Chem. Miner.* 37, 677–684, doi: 10.1007/s00269-010-0367-2.
- Dorogokupets, P.I., Dewaele, A., 2007. Equations of state of MgO, Au, Pt, NaCl–B1, and NaCl–B2: internally consistent high-temperature pressure scales. *High Pressure Res.* 27, 431–446, doi: 10.1080/08957950701659700.
- Dorogokupets, P.I., Oganov, A.R., 2003. Equations of state of Cu and Ag and revised ruby pressure scale. *Dokl. Earth Sci.* 391A (6), 854–857.
- Dorogokupets, P.I., Oganov, A.R., 2004. Intrinsic anharmonicity in equations of state of solids and minerals. *Dokl. Earth Sci.* 395 (2), 238–241.
- Dorogokupets, P.I., Oganov, A.R., 2006. Equations of state of Al, Au, Cu, Pt, Ta, and W and revised ruby pressure scale. *Dokl. Earth Sci.* 410, 1091–1095.
- Dorogokupets, P.I., Oganov, A.R., 2007. Ruby, metals, and MgO as alternative pressure scales: a semiempirical description of shockwave, ultrasonic, X-ray, and thermochemical data at high temperatures and pressures. *Phys. Rev. B* 75, 024115, doi: 10.1103/PhysRevB.75.024115.
- Dorogokupets, P.I., Sokolova, T.S., 2011. Almost absolute equations of state of metals. *Phase Transitions, Ordered States and New Materials*, No. 5, 1–4, <http://ptosnm.ru/catalog/s/67>.
- Dorogokupets, P.I., Sokolova, T.S., Danilov, B.S., Litasov, K.D., 2012. Almost absolute equations of state for diamond, Ag, Al, Au, Cu, Mo, Nb, Pt, Ta, and W for quasi-hydrostatic conditions. *Geodynamics and Tectonophysics* 3, 129–166, <http://dx.doi.org/10.5800/GT-2012-3-2-0067>.
- Dubrovinsky, L.S., Saxena, S.K., 1997. Thermal expansion of periclase (MgO) and tungsten (W) to melting temperatures. *Phys. Chem. Miner.* 24, 547–550.
- Dubrovinsky, L., Boffa-Ballaran, T., Glazyrin, K., Kurnosov, A., Frost, D., Merlini, M., Hanfland, M., Prakapenka, V.B., Schouwink, P., Pippinger, T., Dubrovinskaia, N., 2010. Single-crystal X-ray diffraction at megabar pressures and temperatures of thousands of degrees. *High Pressure Res.* 30, 620–633, doi: org/10.1080/08957959.2010.534092.
- Dubrovinsky, L., Dubrovinskaia, N., Prakapenka, V.B., Abakumov, A.M., 2012. Implementation of micro-ball nanodiamond anvils for high-pressure studies above 6 Mbar. *Nature Communications* 3, 1163, doi: 10.1038/ncomms2160.
- Duffy, T.S., Ahrens, T.J., 1995. Compressional sound velocity equation of state and constitutive response of shock-compressed magnesium oxide. *J. Geophys. Res.* 100B, 529–542, doi: 10.1029/94JB02065.
- Fei, Y., 1999. Effects of temperature and composition on the bulk modulus of (Mg,Fe)O. *Am. Mineral.* 84, 272–276.
- Fei, Y., Li, J., Hirose, K., Minarik, W., Van Orman, J., Sanloup, C., Van Westrenen, W., Komabayashi, T., Funakoshi, K., 2004a. A critical evaluation of pressure scales at high temperatures by in situ X-ray diffraction measurements. *Phys. Earth Planet. Inter.* 143–144, 515–526, doi: 10.1016/j.pepi.2003.09.018.
- Fei, Y., Van Orman, J., Li, J., Van Westrenen, W., Sanloup, C., Minarik, W., Hirose, K., Komabayashi, T., Walter, M., Funakoshi, K., 2004b. Experimentally determined postspinel transformation boundary in Mg₂SiO₄ using MgO as an internal pressure standard and its geophysical implications. *J. Geophys. Res.* 109, B02305, doi: 10.1029/2003JB002562.
- Fei, Y., Ricolleau, A., Frank, M., Mibe, K., Shen, G., Prakapenka, V., 2007. Toward an internally consistent pressure scale. *Proc. Nat. Acad. Sci. USA* 104, 9182–9186.
- Fiquet, G., Richet, P., Montagnac, G., 1999. High-temperature thermal expansion of lime, periclase, corundum and spinel. *Phys. Chem. Miner.* 27, 103–111.
- Fortov, V.E., Lomonosov, I.V., 2010. Shock waves and equations of state of matter. *Shock Waves* 20, 53–71, doi: 10.1007/s00193-009-0224-8.
- Fukui, H., Katsura, T., Kuribayashi, T., Matsuzaki, T., Yoneda, F., Ito, E., Kudoh, Y., Tsutsui, S., Baron, A.Q.R., 2008. Precise determination of elastic constants by high-resolution inelastic X-ray scattering. *J. Synchrotron Radiation* 15, 618–623, doi: 10.1107/S0909049508023248.
- Garai, J., Chen, J., Telekes, G., 2009. The P-V-T equation of state for periclase. *CALPHAD* 33, 737–743, doi: 10.1016/j.calphad.2009.10.001.
- Gerya, T.V., Podlesskii, K.K., Perchuk, L.L., Swamy, V., Kosyakova, N.A., 1998. The equation of state of minerals for petrological bases of thermodynamic data. *Petrologiya* 6 (6), 563–578.
- Gerya, T.V., Podlesskii, K.K., Perchuk, L.L., Maresch, W.V., 2004. Semi-empirical Gibbs free energy formulations for minerals and fluids for use in thermodynamic databases of petrological interest. *Phys. Chem. Miner.* 31, 429–455.
- Guignot, N., Andrault, D., Morard, G., Bolfan-Casanova, N., Mezouar, M., 2007. Thermoelastic properties of post-perovskite phase MgSiO₃ determined experimentally at core-mantle boundary P-T conditions. *Earth Planet. Sci. Lett.* 256, 162–168, doi: 10.1016/j.epsl.2007.01.025.
- Gurvich, L.V., Veits, I.V., Medvedev, V.A., et al., 1981. *Thermodynamic Properties of Substances [in Russian]*. Nauka, Moscow, Vol. 3, Book 2.
- Hama, J., Suito, K., 1999. Thermoelastic properties of periclase and magnesio-wüstite under high pressure and high temperatures. *Phys. Earth Planet. Inter.* 114, 165–179.
- Heinz, D., Jeanloz, R., 1984. Compression of the B2 high-pressure phase of NaCl. *Phys. Rev. B* 30, 6045–6050.
- Hemley, R.J., Percy, W., 2010. Bridgman's second century. *High Pressure Res.* 30, 581–619, doi: org/10.1080/08957959.2010.538974.
- Hirose, K., Sata, N., Komabayashi, Y., Ohishi, Y., 2008. Simultaneous volume measurements of Au and MgO to 140 GPa and thermal equation of state of Au based on the MgO pressure scale. *Phys. Earth Planet. Inter.* 167, 149–154, doi: 10.1016/j.pepi.2008.03.002.
- Hixson, R.S., Fritz, J.N., 1992. Shock compression of tungsten and molybdenum. *J. Appl. Phys.* 71, 1721–1728.
- Holland, T.J.B., Powell, R., 1998. An internally-consistent thermodynamic dataset for phases of petrological interest. *J. Metam. Geol.* 16, 309–344.
- Holland, T.J.B., Powell, R., 2011. An improved and extended internally consistent thermodynamic dataset for phases of petrological interest, involving a new equation of state for solids. *J. Metam. Geol.* 29, 333–383.
- Holmes, N., Moriarty, J., Gather, G., Nellis, W., 1989. The equation of state of platinum to 660 GPa (6.6 Mbar). *J. Appl. Phys.* 66, 2962–2967.
- Holzappel, W.B., 2001. Equations of state for solids under strong compression. *Z. Kristallogr.* 216, 473–488.

- Holzappel, W.B., 2003. Refinement of ruby luminescence pressure scale. *J. Appl. Phys.* 93, 1813–1818.
- Holzappel, W.B., 2005. Progress in the realization of a practical pressure scale for the range 1–300 GPa. *High Pressure Res.* 25, 87–96.
- Holzappel, W.B., 2010. Equations of state for Cu, Ag, and Au and problems with shock wave reduced isotherms. *High Pressure Res.* 30, 372–394, doi: 10.1080/08957959.2010.494845.
- Inbar, I., Cohen, R.E., 1995. High pressure effects on thermal properties of MgO. *Geophys. Res. Lett.* 22 (12), 1533–1536, doi: 10.1029/95GL01086.
- Inoue, T., Irifune, T., Higo, Y., Sanehira, T., Sueda, Y., Yamada, A., Shinmei, T., Yamazaki, D., Ando, J., Funakoshi, K., Utsumi, W., 2006. The phase boundary between wadsleyite and ringwoodite in Mg₂SiO₄ determined by in situ X-ray diffraction. *Phys. Chem. Miner.* 33, 106–114, doi: 10.1007/s00269-005-0053-y.
- Isaak, D.G., Anderson, O.L., Goto, T., 1989. Measured elastic moduli of single-crystal MgO up to 1800 K. *Phys. Chem. Miner.* 16, 704–713.
- Isaak, D.G., Cohen, R.E., Mehl, M.J., 1990. Calculated elastic and thermal properties of MgO at high pressures and temperatures. *J. Geophys. Res.* 95, 7055–7067.
- Jackson, I., Niesler, H., 1982. The elasticity of periclase to 3 GPa and some geophysical implications, in: Akimoto, S., Manghnani, M.H. (Eds.), *High Pressure Research in Geophysics*. Center of Academic Publications of Japan, Tokyo, pp. 98–113.
- Jacobs, M.H.G., de Jong, B.H.W.S., 2003. The high-temperature and high-pressure behavior of MgO derived from lattice vibration calculations. Kieffer's model revised. *Phys. Chem. Chem. Phys.* 5, 2056–2065, doi: 10.1039/b301550e.
- Jacobs, M.H.G., Oonk, H.A.J., 2000. A realistic equation of state for solids. The high pressure and high temperature thermodynamic properties of MgO. *CALPHAD* 24, 133–147.
- Jacobsen, S.D., Holl, C.M., Adams, K.A., Fischer, R.A., Martin, E.S., Bina, C.R., Lin, J.F., Prakapenka, V.B., Kubo, A., Dera, P., 2008. Compression of single-crystal magnesium oxide to 118 GPa and a ruby pressure gauge for helium pressure media. *Am. Mineral.* 93, 1823–1828.
- Jamieson, J.C., Fritz, J.N., Manghnani, M.H., 1982. Pressure measurement at high temperature in X-ray diffraction studies: gold as a primary standard, in: Akimoto, S., Manghnani, M.H. (Eds.), *High Pressure Research in Geophysics*. Center of Academic Publications of Japan, Tokyo, pp. 27–48.
- Jin, K., Li, X., Wu, Q., Geng, H., Cai, L., Zhou, X., Jing, F., 2010. The pressure-volume-temperature equation of state of MgO derived from shock Hugoniot data and its application as a pressure scale. *J. Appl. Phys.* 107, 113518, doi: 10.1063/1.3406140.
- Jin, K., Wu, Q., Geng, H., Li, X., Cai, L., Zhou, X., 2011. Pressure-volume-temperature equations of state of Au and Pt up to 300 GPa and 3000 K: internally consistent pressure scales. *High Pressure Res.* 31, 560–580, doi: 10.1080/08957959.2011.611469.
- Kennett, B.L.N., Jackson, I., 2009. Optimal equations of state for mantle minerals from simultaneous non-linear inversion of multiple datasets. *Phys. Earth Planet. Inter.* 176, 98–108, doi: 10.1016/j.pepi.2009.04.005.
- Klotz, S., Chervin, J.-C., Munsch, P., Le Marchand, G., 2009. Hydrostatic limits of 11 pressure transmitting media. *J. Phys. D: Appl. Phys.* 42, 075413, doi: 10.1088/0022-3727/42/7/075413.
- Knopoff, I., 1965. Approximate compressibility of elements and compounds. *Phys. Rev.* 138 (5A), A1445–A1447.
- Komabayashi, T., Hirose, K., Sugimura, E., Sata, N., Ohishi, Y., Dubrovinsky, L.S., 2008. Simultaneous volume measurements of post-perovskite and perovskite in MgSiO₃ and their thermal equations of state. *Earth Planet. Sci. Lett.* 265, 515–524, doi: 10.1016/j.epsl.2007.10.036.
- Kono, Y., Irifune, T., Higo, Y., Inoue, T., Barnhoorn, A., 2010. P-V-T relation of MgO derived by simultaneous elastic wave velocity and in situ X-ray measurements: a new pressure scale for the mantle transition region. *Phys. Earth Planet. Inter.* 183, 196–211, doi: 10.1016/j.pepi.2010.03.010.
- Kuskov, O.L., Galimzyanov, R.F., Kalinin, V.A., 1982. Construction of a thermal equation of state for solid phases (periclase, coesite, stishovite) from their compression moduli and calculation of the coesite-stishovite phase equilibrium. *Geokhimiya*, No. 7, 984–1001.
- Lakshtanov, D.L., Sinogeikin, S.V., Sanchez-Valle, C., Prakapenka, V., Shen, G., Gregoryanz, E., Bass, J.D., 2005. Aggregate elastic moduli and equation of state of B2 phase of NaCl to 73 GPa by simultaneous synchrotron X-ray diffraction and Brillouin scattering measurements. *EOS Trans. AGU* 86 (52), Fall Meet. Suppl., MR31A-0114.
- Levashov, P.R., Khishchenko, K.V., Lomonosov, I.V., Fortov, V.E., 2004. Database on shock-wave experiments and equations of state available via Internet. *Am. Inst. Phys. Conf. Proc.* 706, 87–90, <http://teos.ficp.ac.ru/rusbank/>, <http://www.ihed.ras.ru/rusbank/>
- Li, B.S., Woody, K., Kung, J., 2006. Elasticity of MgO to 11 GPa with an independent absolute pressure scale: implications for pressure calibration. *J. Geophys. Res.* 111, B11206, doi: 10.1029/2005JB004251.
- Litasov, K.D., 2011. Physicochemical conditions for melting in the Earth's mantle containing a C–O–H fluid (from experimental data). *Russian Geology and Geophysics (Geologiya i Geofizika)* 52 (5), 475–492 (613–635).
- Litasov, K.D., Ohtani, E., Sano, A., Suzuki, A., Funakoshi, K., 2005. In situ X-ray diffraction study of post-spinel transformation in a peridotite mantle: implication for the 660-km discontinuity. *Earth Planet. Sci. Lett.* 238 (3–4), 311–328.
- Litasov, K.D., Shatskiy, A., Fei, Y., Suzuki, A., Ohtani, E., Funakoshi, K., 2010. Pressure-volume-temperature equation of state of tungsten carbide to 32 GPa and 1673 K. *J. Appl. Phys.* 108, 053513, doi: 10.1063/1.3481667.
- Mao, H.K., Bell, P.M., Shaner, J.W., Steinberg, D.J., 1978. Specific volume measurements of Cu, Mo, Pd, and Ag and calibration of the ruby R1 fluorescence pressure gauge from 0.06 to 1 Mbar. *J. Appl. Phys.* 49, 3276–3283.
- Mao, H.K., Xu, J., Bell, P.M., 1986. Calibration of the ruby pressure gauge to 800 kbar under quasi-hydrostatic conditions. *J. Geophys. Res.* 91B, 4673–4676.
- Marsh, S.P., 1980. *LASL Shock Hugoniot Data*. Univ. California Press, Berkeley.
- Martinez-Garcia, D., Le Codec, Y., Mezouar, M., Syfosse, G., Itie, J.P., Besson, J.M., 2000. Equation of state of MgO at high pressure and temperature. *High Pressure Res.* 18, 339–344.
- Matsui, M., Nishiyama, N., 2002. Comparison between the Au and MgO pressure calibration standards at high temperature. *Geophys. Res. Lett.* 29, 1368, doi: 10.1029/2001GL014161.
- Matsui, M., Parker, S.C., Leslie, M., 2000. The MD simulation of the equation of state of MgO as a pressure calibration standard at high temperature and high pressure. *Am. Mineral.* 85, 312–316.
- Matsui, M., Ito, E., Katsura, T., Yamazaki, D., Yoshino, T., Yokoyama, A., Funakoshi, K., 2009. The temperature-pressure-volume equation of state of platinum. *J. Appl. Phys.* 105, 013505, doi: 10.1063/1.3054331.
- Molodets, A.M., Shakhrai, D.V., Golyshev, A.A., Babare, L.V., Avdonin, V.V., 2006. Equation of state of solids from high-pressure isotherm. *High Pressure Res.* 26, 223–231, doi: 10.1080/08957950600864369.
- Ocelli, F., Loubeyre, P., LeToullec, R., 2003. Properties of diamond under hydrostatic pressures up to 140 GPa. *Nature Mater.* 2, 151–154, doi: 10.1038/nmat831.
- Oganov, A.R., Dorogokupets, P.I., 2003. All-electron and pseudopotential study of MgO: equation of state, anharmonicity, and stability. *Phys. Rev. B* 67, 224110, doi: 10.1103/PhysRevB.67.224110.
- Oguri, K., Funamori, N., Uchida, T., Miyajima, N., Yagi, T., Fujino, K., 2000. Post-garnet transition in a natural pyrope: a multi-anvil study based on in situ X-ray diffraction and transmission electron microscopy. *Phys. Earth Planet. Inter.* 122, 175–186.
- Ono, S., Kikegawa, T., Ohishi, Y., 2006. Structural property of CsCl-type sodium chloride under pressure. *Solid State Communications* 137, 517–521, doi: 10.1016/j.ssc.2006.01.022.
- Ono, S., Brodholt, J.P., Alfe, D., Alfredson, M., Price, G.D., 2008. Ab initio molecular dynamics simulations for thermal equation of state of B2-type NaCl. *J. Appl. Phys.* 103, 023510, doi: 10.1063/1.2832632.
- Ono, S., Kikegawa, T., Hirao, N., Mibe, K., 2010. High-pressure magnetic transition in hcp-Fe. *Am. Mineral.* 95, 880–883, doi: 10.2138/am.2010.3430.
- Otero-de-la-Rosa, A., Luana, V., 2011a. Treatment of first-principles data for predictive quasiharmonic thermodynamics of solids: the case of MgO. *Phys. Rev. B* 84, 024109, doi: 10.1103/PhysRevB.84.024109.

- Otero-de-la-Rosa, A., Luana, V., 2011b. Equations of state and thermodynamics of solids using empirical corrections in the quasiharmonic approximation. *Phys. Rev. B* 84, 184103, doi: 10.1103/PhysRevB.84.184103.
- Pan'kov, V., Kalinin, V.A., 1974. The equations of state for mineral-forming oxides. *Izv. Akad. Nauk SSSR. Ser. Fizika Zemli*, No. 3, 3–13.
- Polyakov, V.B., Kuskov, O.L., 1994. Self-consistent model for calculation of the thermoelastic and caloric properties of minerals. *Geokhimiya*, No. 7, 1096–1122.
- Reeber, R.R., Goessel, K., Wang, K., 1995. Thermal expansion and molar volume of MgO, periclase, from 5 to 2900 K. *Eur. J. Mineral.* 7, 1039–1047.
- Ruoff, A.L., 1967. Linear shock-velocity-particle-velocity relationship. *J. Appl. Phys.* 38, 4976–4980.
- Ruoff, A.L., Xia, H., Xia, Q., 1992. The effect of a tapered aperture on X-ray diffraction from a sample with a pressure gradient: studies on three samples with a maximum pressure of 560 GPa. *Rev. Sci. Instrum.* 63, 4342–4348, doi: 10.1063/1.1143734.
- Sakai, T., Ohtani, E., Hirao, N., Ohishi, Y., 2011a. Equation of state of the NaCl-B2 phase up to 304 GPa. *J. Appl. Phys.* 109, 084912, doi: 10.1063/1.3573393.
- Sakai, T., Ohtani, E., Hirao, N., Ohishi, Y., 2011b. Stability field of the hcp-structure for Fe, Fe-Ni, and Fe-Ni-Si alloys up to 3 Mbar. *Geophys. Res. Lett.* 38, L09302, doi: 10.1029/2011GL047178.
- Sata, N., Shen, G., Rivers, M.L., Sutton, S.R., 2002. Pressure-volume equation of state of the high-pressure B2 phase of NaCl. *Phys. Rev. B* 65, 104114.
- Sata, N., Hirose, K., Shen, G., Nakajima, Y., Ohishi, Y., Hirao, N., 2010. Compression of FeSi, Fe₃C, Fe_{0.95}O, and FeS under the core pressures and implication for light element in the Earth's core. *J. Geophys. Res.* 115, B09204, doi: 10.1029/2009JB006975.
- Seagle, C.T., Campbell, A.J., Heinz, D.L., Shen, G., Prakapenka, V.B., 2006. Thermal equation of state of Fe₃S and implications for sulfur in Earth's core. *J. Geophys. Res.* 111, B06209, doi: 10.1029/2005JB004091.
- Shim, S.H., Duffy, T.S., Kenichi, T., 2002. Equation of state of gold and its application to the phase boundaries near 660 km depth in Earth's mantle. *Earth Planet. Sci. Lett.* 203, 729–739.
- Silvera, I.F., Chijioke, A.D., Nellis, W.J., Soldatov, A., Tempere, J., 2007. Calibration of the ruby pressure scale to 150 GPa. *Phys. Stat. Solidi B* 244, 460–467, doi: 10.1002/pssb.200672587.
- Sinogeikin, S.V., Bass, J.D., 2000. Single-crystal elasticity of pyrope and MgO to 20 GPa by Brillouin scattering in the diamond cell. *Phys. Earth Planet. Inter.* 120, 43–62.
- Sinogeikin, S.V., Jackson, J.M., O'Neill, B., Palko, J.W., Bass, J.D., 2000. Compact high-temperature cell for Brillouin scattering measurement. *Rev. Sci. Instrum.* 71 (1), 201–206.
- Sokolova, T.S., Dorogokupets, P.I., 2011. The equation of state for gold. *Phase Transitions, Ordered States and New Materials*, No. 5, 1–4. <http://ptosnm.ru/catalog/s/67>.
- Spetzler, H., 1970. Equation of state of poly-crystalline and single-crystal MgO to 8 kilobars and 800 K. *J. Geophys. Res.* 75, 2073–2087.
- Speziale, S., Zha, C., Duffy, T.S., Hemley, R.J., Mao, H.K., 2001. Quasi-hydrostatic compression of magnesium oxide to 52 GPa: implications for the pressure-volume-temperature equation of state. *J. Geophys. Res.* 106B, 515–528.
- Stamenkovic, V., Breuer, D., Spohn, T., 2012. Thermal and transport properties of mantle rock at high pressure: Applications to super-Earths. *Icarus* 216, 572–596, doi: 10.1016/j.icarus.2011.09.030.
- Stixrude, L., Lithgow-Bertelloni, C., 2005. Thermodynamics of mantle minerals—I. Physical properties. *Geophys. J. Int.* 162, 610–632, doi: 10.1111/j.1365-246X.2005.02642.x.
- Sumino, Y., Anderson, O.L., Suzuki, I., 1983. Temperature coefficients of elastic constants of single crystal MgO between 80 and 1300 K. *Phys. Chem. Miner.* 9, 38–47.
- Sun, T., Umamoto, K., Wu, Z., Zheng, J.-C., Wentzcovitch, R.M., 2008. Lattice dynamics and thermal equation of state of platinum. *Phys. Rev. B* 78, 024304, doi: 10.1103/PhysRevB.78.024304.
- Svendsen, B., Ahrens, T.J., 1987. Shock-induced temperatures of MgO. *Geophys. J. R. Astr. Soc.* 91, 667–691.
- Syassen, K., 2008. Ruby under pressure. *High Pressure Res.* 28, 75–126, doi: 10.1080/08957950802235640.
- Takemura, K., 2001. Evaluation of the hydrostaticity of a helium-pressure medium with powder X-ray diffraction techniques. *J. Appl. Phys.* 89, 662–668, doi: 10.1063/1.1328410.
- Takemura, K., Dewaele, A., 2008. Isothermal equation of state for gold with a He-pressure medium. *Phys. Rev. B* 78, 104119, doi: 10.1103/PhysRevB.78.104119.
- Takemura, K., Singh, A.K., 2006. High-pressure equation of state for Nb with a helium-pressure medium: powder x-ray diffraction experiments. *Phys. Rev. B* 73, 224119, doi: 10.1103/PhysRevB.73.224119.
- Tang, L.-Y., Liu, L., Liu, J., Xiao, W., Li, Y.-C., Li, X.-D., Bi, Y., 2010. Equation of state of tantalum up to 133 GPa. *Chin. Phys. Lett.* 27, 016402, doi: 10.1088/0256-307X/27/1/016402.
- Tange, Y., Nishihara, Y., Tsuchiya, T., 2009. Unified analyses for *P-V-T* equation of state of MgO: a solution for pressure-scale problems in high *P-T* experiments. *J. Geophys. Res.* 114, B03208, doi: 10.1029/2008JB005813.
- Tateno, S., Hirose, K., Sata, N., Ohishi, Y., 2009. Determination of post-perovskite phase transition boundary up to 4400 K and implications for thermal structure in D'' layer. *Earth Planet. Sci. Lett.* 277, 130–136.
- Tateno, S., Hirose, K., Ohishi, Y., Tatsumi, Y., 2010. The structure of iron in Earth's inner core. *Science* 330, 359–361, doi: 10.1126/science.1194662.
- Ueda, Y., Matsui, M., Yikoyama, A., Tange, Y., Funakoshi, K.-I., 2008. Temperature-pressure-volume equation of state of the B2 phase of sodium chloride. *J. Appl. Phys.* 103, 113513, doi: 10.1063/1.2939254.
- Utsumi, W., Weidner, D.J., Liebermann, R.C., 1998. Volume measurement of MgO at high pressures and temperatures, in: Manghnani, M.H., Yagi, T. (Eds.), *Properties of Earth and Planetary Materials at High Pressure and Temperature*. *Geophys. Monogr. Ser.* 101, AGU, Washington, D.C., pp. 327–333.
- Vassiliou, M.S., Ahrens, T.J., 1981. Hugoniot equation of state of periclase to 200 GPa. *Geophys. Res. Lett.* 8, 729–732.
- Vinet, P., Ferrante, J., Rose, J.H., Smith, J.R., 1987. Compressibility of solids. *J. Geophys. Res.* 92, 9319–9325.
- Wu, Z., Wentzcovitch, R.M., Umamoto, K., Li, B., Hirose, K., Zheng, J.-C., 2008. Pressure-volume-temperature relations in MgO: an ultrahigh pressure-temperature scale for planetary sciences applications. *J. Geophys. Res.* 113, B06204, doi: 10.1029/2007JB005275.
- Yokoo, M., Kawai, N., Nakamura, K.G., Kondo, K., 2008. Hugoniot measurement of gold at high pressures of up to 580 GPa. *Appl. Phys. Lett.* 92, 051901, doi: 10.1063/1.2840189.
- Yokoo, M., Kawai, N., Nakamura, K.G., Kondo, K., Tange, Y., Tsuchiya, T., 2009. Ultrahigh-pressure scales for gold and platinum at pressures up to 550 GPa. *Phys. Rev. B* 80, 104114, doi: 10.1103/PhysRevB.80.104114.
- Zha, C.-S., Mao, H.K., Hemley, R.J., 2000. Elasticity of MgO and a primary pressure scale to 55 GPa. *Proc. Nat. Acad. Sci. USA* 97, 13,494–13,499.
- Zha, C.-S., Mibe, K., Bassett, W.A., Tschauer, O., Mao, H.K., Hemley, R.J., 2008. *P-V-T* equation of state of platinum to 80 GPa and 1900 K from internal resistive heating/X-ray diffraction measurement. *J. Appl. Phys.* 103 (5), 054908, doi: 10.1063/1.2844358.
- Zhang, H., Bukowinski, M.S.T., 1991. Modified potential-induced-breathing model of potentials between close-shell ions. *Phys. Rev. B* 44 (6), 2495–2503.
- Zhang, L., Gong, Z., Fei, Y., 2008. Shock-induced phase transitions in the MgO-FeO system to 200 GPa. *J. Phys. Chem. Solids* 69, 2344–2348.
- Zharkov, V.N., Kalinin, V.A., 1968. *Equations of State for Solids at High Pressures and Temperatures* [in Russian]. Nauka, Moscow.